# EVENT-BASED URBAN FLOOD MODELLING WITH SWMM PROGRAM

**Seid Dessalegn SHAFI**

**Master's Thesis**

**Department of Civil Engineering**

**Programme in Hydraulics**

**Supervisor: Prof. Dr. Mustafa TOMBUL**

**Eskişehir**

**Eskişehir Technical University**

**Institute of Graduate Programs**

**April 2022**

# ABSTRACT

EVENT-BASED URBAN FLOOD MODELLING WITH SWMM PROGRAM

Seid Dessalegn SHAFI

Department of Civil Engineering

Programme in Hydraulics

Eskişehir Technical University, Institute of Graduate Programs, April 2022

Supervisor: Prof. Dr. Mustafa TOMBUL

Urban stormwater management is a significant tool in flood analysis and estimating the capacity of a drainage system. Engineers frequently use mathematical modeling of watersheds to solve urban flooding problems. Stormwater modeling is the quantitative analysis and exploration of novel stormwater design solutions by designers. The USEPA Storm Water Management Model (SWMM), (PCSWMM), (QQS), (DR3M), (HEC-HMS), and MIKE URBAN are just a few of the mathematical modeling tools widely used to address urban flooding issues.

The purpose of this project is to develop, adjust, and evaluate an urban event-based rainfall-runoff model for the Boğaziçi neighborhood in the Mamak district of Ankara province, Turkey, using old (2018 and before ) and current infrastructural networks. Additionally, the current drainage system was simulated based on design storms with return periods of 2, 5, 10, 50, and 100 years. Three alternative scenarios with two different rainfall events were used to examine the drainage network's response.

The results of three alternative scenarios, based on different indexes for urban flood forecasting, show that the fundamental problem with old drainage was an insufficient drainage infrastructure. The Rational method was used to estimate peak discharges for comparison and evaluation purpose with simulated values from SWMM . The result of different measurments for model evaluation shows that result shows that the model performs quite well.

**Keywords:** Urban Flood Modeling, Stormwater Modeling, Mathematical Modeling, EPA-SWMM

# ÖZET

SWMM PROGRAMI KULLANARAK OLAY TABANLI KENTSEL TAŞKIN MODELLEMESİ



Seid Dessalegn SHAFI

İnşaat Mühendisliği Anabilim Dalı

Hidrolik Bilim Dalı

Eskişehir Teknik Üniversitesi, Lisansüstü Eğitim Enstitüsü,

Danışman: Prof. Dr. Mustafa TOMBUL


Kentsel yağmur suyu yönetimi, bir drenaj sisteminin kapasitesinin taşkın analizi ve tahmininde önemli bir araçtır. Mühendisler genellikle kentsel sel problemlerini çözmek için su havzalarının matematiksel modellemesini kullanırlar. Yağmur suyu modellemesi, tasarımcılar tarafından yeni yağmur suyu tasarım çözümlerinin nicel analizi ve keşfidir. USEPA Yağmursuyu Yönetim Modeli (SWMM), (PCSWMM), (QQS), (DR3M), (HEC-HMS), ve MIKE URBAN kentsel sel sorunlarını ele almak için yaygın olarak kullanılan matematiksel modelleme araçlarından sadece birkaçıdır.

Bu projenin amacı, Türkiye'nin Ankara ilinin Mamak ilçesindeki Boğaziçi mahallesi için geçmişteki (2018 ve önceki) ve mevcut altyapı ağlarını kullanarak bir kentsel olay tabanlı yağış-akış modeli geliştirmek, ayarlamak ve değerlendirmektir. Ek olarak, mevcut drenaj sistemi 2, 5, 10, 50 ve 100 yıllık tekerrürlü yağışlara dayalı olarak simüle edilmiştir. Drenaj ağının tepkisini incelemek için iki farklı yağış olayının olduğu üç ayrı senaryo kullanılmıştır.

Kentsel sel tahmini için farklı endekslere dayanan üç alternatif senaryonun sonuçları, geçmişteki drenajla ilgili temel sorunun yetersiz drenaj altyapısı olduğunu göstermektedir. Rasyonel yöntemi, SWMM'den alınan simüle edilmiş değerlerle karşılaştırma ve değerlendirme amacıyla pik deşarjları tahmin etmek için kullanılmıştı. Model değerlendirmesi için farklı ölçümlerin sonucu, modelin oldukça iyi performans gösterdiğini göstermektedir.



**Anahtar Kelimeler:** Kentsel Taşkın Modelleme, Yağmursuyu Modelleme, Matematiksel Modelleme, EPA-SWMM

**ACKNOWLEDGEMENTS**

All praise is devoted to Allah, the All-Mighty, the Most Merciful, who taught man what he did not know.

I would like to express my sincere gratitude to my adviser, **Prof. Dr. Mustafa TOMBUL**, who never left me professionally or morally during the process of my thesis. I am thankful to you for your encouragement, love, and support.

I would want to express my heartfelt gratitude to everyone who contributed to my thesis, primarily my mother and father. Without their encouragement and assistance, this thesis would not have been completed. Finally, I'd want to express my deepest gratitude to **Assoc.Prof. Sezar GÜLBAZ**, who assisted me tremendously with my thesis.

Seid DessalegnSHAFI

## STATEMENT OF COMPLIANCE WITH ETHICAL PRINCIPLES AND RULES

I hereby truthfully declare that this thesis is an original work prepared by me; that I have behaved in accordance with the scientific ethical principles and rules throughout the stages of preparation, data collection, analysis and presentation of my work; that I have cited the sources of all the data and information that could be obtained within the scope of this study, and included these sources in the references section; and that this study has been scanned for plagiarism with “scientific plagiarism detection program” used by Eskişehir Technical University, and that “it does not have any plagiarism” whatsoever. I also declare that, if a case contrary to my declaration is detected in my work at any time, I hereby express my consent to all the ethical and legal consequences that are involved.

Seid Dessalegn SHAFI

CONTENTS

**Page**

## LIST OF TABLES

**Page**

# LIST OF FIGURES

**Page**

## GLOSSARY OF SYMBOL AND ABREVATION

| | | |
|---|---|---|
| A | : | Catchment Area |
| $A°$ | : | Cross-sectional Area of Flow |
| C° | : | Conduits |
| C | : | Runoff Coefficent |
| d | : | Index of Agrrement |
| DL | : | Dublex |
| e | : | Rate of Surface Evaporation |
| f | : | Rate of infiltration |
| g | : | Gravitional Accleration |
| H | : | Water Hydraulic Head |
| ha | : | Hectare |
| hr | : | Hour |
| i | : | Rainfall and Snowmelt Rate |
| J | : | Junction |
| d | : | Index of Agrrement |
| L | : | Low |
| M | : | Medium |
| m | : | Meter |
| mm | : | Mili-Meter |
| n | : | Manning Coeeficent |
| n° | : | Number in dataset |
| P | : | Park |
| $P_i$ | : | Forcast Value |
| $Q_0$ | : | Measured Discharge |
| $Q_i$ | : | Observation value |
| $Q_s$ | : | Simulated Discharge |
| Q | : | Flow Rate |
| q | : | Runoff rate |
| R | : | Hydraulic Radius |

| | | |
|---|---|---|
| r | : | Pearson Coorelation |
| s | : | Second |
| S | : | Subcatchment |
| $S^0$ | : | Slope |
| $S_f$ | : | Friction Coefficent |
| t | : | Time |
| X | : | Observed Data |
| x | : | Distance |
| Y | : | Water Depth |
| y | : | Modeled Data |
| Z | : | Inverted Elevation |
| A | : | Appendix |
| ARC-GIS | : | Aeronautical Reconnaissance Coverage Geographic Information System |
| ASKI | : | Ankara Su ve Kanalizasyon İdaresi Genel Müdürlüğü |
| CAD | : | Computer Aided Disgn |
| DEM | : | Digital elevation map |
| DR3M | : | Distributee Routing Rainfall-Runoff Model |
| EM-DAT | : | Emergency Events Database |
| GIS | : | Geographic Information System |
| HEC-HMS | : | Hydrologic Engineering Centere's Hydraulic Modeling System |
| HSPF | : | Hydrologic Simulation Program-FORTRAN |
| ID | : | Identity |
| IDF | : | Intensity-Duration-Frequency |
| LID | : | Low Impact Development |
| MAE | : | Mean Absolute Error |
| M/D/Y | : | Month/Day/Year |
| NSE | : | Nash and Sutellitte Efficiency |
| PCSWMM | : | Personal Computer Storm Water Managment Model |
| PVC | : | PolyVinyl chloride |
| QQS | : | Quality-Quantity Simulation |

| | | |
|---|---|---|
| RMSE | : | Root Mean Square Error |
| STORM | : | Storage Treatment Overflow Runoff Model |
| SWMM | : | Storm Water Managment Model |
| USEPA | : | United States Enviromental Protection Agency |
| USGS | : | United States Geologocal Survey |
| XLS | : | Computer Aided Disgn |
| XP SWMM | : | XP Stormwater Wastewater mangment model |
| 1-D | : | 1 Dimensional |

# 1. INTRODUCTION

Urban flooding occurs primarily in developed areas when a drainage system's capacity is insufficient to handle rainwater runoff or water does not infiltrate into the ground. It differs from rural flooding in that urbanization causes the formation of catchments, resulting in an increase in flood peaks and flood volumes. Urban flooding is predominantly the result of a combination of factors, including heavy rainfall, residential and commercial development in floodplains, high coverage of impermeable areas, and an insufficient drainage system that results in excessive runoff in developed areas where water has nowhere to go (Kömüşcü & Çelik, 2013). Climate change, by altering precipitation patterns, also makes a significant contribution to urban flooding.

Engineers frequently use mathematical modeling of watersheds to identify solutions to flooding problems. With a model that accurately represents the events under analysis, this type of watershed modeling requires data to calibrate and validate the model's outputs. Adequate resources are required for the acquisition of the data and model on both a physical and financial level. The (USEPA) Storm Water Management Model (SWMM), (PCSWMM), MIKE URBAN, (QQS), (DR3M), and (HEC HMS) are just a few of the mathematical modeling packages that are frequently used to solve urban flooding problems (Wanniarachchi & Wijesekera, 2012). These models calculate flood peaks and design drainage systems using a variety of mathematical formulas.

Stormwater modeling is the mathematical modeling that enables designers to analyze and explore innovative stormwater design options and efficiently manage project deliverables. Effective stormwater management is an important part of land development and roadway design projects and is an essential aspect of public service in any community. Designing an effective system requires balancing the design between oversizing, which increases capital budgets, and under-sizing, which can lead to potential flooding problems. Using hydrologic and hydraulic terms helps to understand how rainfall translates into stormwater runoff and interacts with streets, channels, pipes, ponds, and other related stormwater infrastructure. Surface channels must be properly sized and aligned in order to alleviate flooding problems.

## 1.1 Background

After earthquakes, floods are the most destructive type of natural disaster in Turkey (EM-DAT, 2012). The biggest cause of floods and overflows in Turkey is climatic conditions. Both human and geographical factors are important factors in the occurrence of floods and overflows. Heavy rainfall lasting for days in April and May causes floods in some places. Ankara, the capital of Turkey, is one of the most affected cities by the stormwater floods. Heavy rains in Ankara always occur in these periods, in convectional (short-term and limited area) form. The flood disaster, which caused the most loss of life in the history of the Turkish Republic, occurred in the Hatip Stream valley of Ankara in September 1957 and resulted in the deaths of 185 people. Flood disasters in Turkey are the natural disasters that cause the greatest economic losses. According to the 2002 inventory data, the economic damage caused by the floods reaches an average of 100,000,000 USD per year (Toros et al., 2018)

## 1.2. Project Aim and Purpose

The aim of the project is to establish, adjust and callibrate an urban event-based rainfall-runoff model based on old (2018 and before ) and current infrastructure networks for the Boğaziçi neighborhood in the Mamak district of Ankara province, Turkey, based on the flood that occurred in May 2018. In addition, different datasets, such as rainfall data from different storm events, will be used in accessing the performance of the drainage system. Finally, different modifications will be applied to improve the effectiveness of the drainage networks in the research area.

The purpose of this project is to combine urban flood simulation models with different model evaluation and efiicency criterias in order to analyze the current performance of drainage systems in the context of stormwater excess management.

## 1.3. Limitation

Some limitations that come across to make the project more intensive and comprehensive are described as follows:

a) Since there are no clear rules for the division of sub-catchment areas, it is difficult to decide which method is best to get a better result.
b) Like most models, this model takes the mean slope as the slope parameter of the sub-basin area, which introduces errors in a mechanism in the model.

c) Hydrograph calibration was not performed due to the lack of observed flow data for the discharge of the study area.

## 1.4. Previous Research Projects

Some previous research related to urban flood modeling using the SWMM package and its comparison with other software has been approved and published. However, those research projects vary in the focus of the discussions, objectives, and case studies.

S. Wanniarachchi and N. T. S. Wijesekera (2016) used SWMM to manage floodplains in an unmeasured urban watershed. The authors concluded in this report that SWMM is applicable to the ungauged urban flood modeling of the Matara City Council. This study utilized published values and data collected during field visits for flow modeling in order to obtain an order of magnitude with which to compare engineering alternatives for stormwater management (Wanniarachchi & Wijesekera, 2012).

Haris et al. (2016) compared some urban stormwater management software based on functionality, availability, characteristics, and components in analyzing the quality of representative models. The EPA SWMM is publicly accessible and can be used for planning and design functions. However, other software such as HEC-HMS can only be used for operational purposes (Haris et al., 2016)

M.L. Waikarand and Undegaonkar Namita (2015) used EPA SWMM 5 to model an urban flood on an education campus in Nanded, Vishnupuri.This research concluded that EPA SWMM 5 is capable of simulating a watershed's response to rainfall events and generating runoff, a water depth profile, and an outflow hydrograph. It also used a rational formula to figure out the runoff (Waikar & Namita, 2015)

In 2014, Lei Jiang et al. conducted an urban flood simulation model using SWMM to analyze urban flood simulation in the rapidly urbanizing city of Dongguan, southern China. The research concluded that the SWMM model is possibly suitable for urban flood prediction. However, some limitations of SWMM were also observed during this research. These limitations are generally associated with the lack of surface runoff routing in SWMM, which makes it difficult to predict urban flooding with precision (Jiang et al., 2015).

According to Kourtis et al. (2017), the SWMM model can accurately simulate the shape of the hydrograph, the peak discharge, and the peak time for both calibration and validation events in the combined drainage network. Using the SWMM model as a whole has been found to be a very good way to model urban drainage networks (Kourtis et al., 2017)

Junaidi et al. (2018) evaluated the drainage system surrounding Padang's Sungai Sapih district hospital in 2018 by calculating the quality and quantity of runoff from each catchment area, as well as the runoff, the depth of runoff, and the water quality in each pipeline and drainage channel throughout the simulation period. Additionally, this study determined that the drainage planning design for the study region is insufficient to support the area's drainage load today and, in the future (Junaidi et al., 2018).

Sunny Agarwal and Sanjeet Kumar, 2020, analyzed urban flood modeling using SWMM for historical and future extreme storm events under the climate change scenario. In the study, it was concluded that flooding occurred at several nodes in the region and that there were some overflow sections. This overflow in sections and nodes is due to heavy precipitation and the impermeability of the surface. In addition, such a project is beneficial for policy makers to assess future floods, reduce the risk of urban flooding, and design an appropriate urban drainage system in developing urban cities (Agarwal & Kumar, 2020)

# 2. LITERATURE REVIEW AND THEORETICAL BASE

## 2.1. General Description of a Mathematical Model

The reason for using the model is the complexity caused by the real-world system, which makes it difficult to reflect reality at that certain moment. A model has different forms, either physically or mathematically. A physical analogy for operating a system is provided by the physical model, and in most cases, it is not possible to physically represent it. In this context, another type of model called the "mathematical model" will be emphasized. In a hydrological system, one cannot normally physically model a watershed or precipitation. That is, all hydrological models are mathematical models that use mathematical equations that characterize the prototype system and provide the relationships between variables that provide definition, analysis, and prediction under the conditions to be modeled (Öner, 1997).

While there are many different types of mathematical models, they all share a fundamental principle in that they allow for the examination of a system in order to evaluate its performance. Depending on the performance of the system, the person using the model determines whether the system will work at the desired level. On the other hand, an acceptable level of accuracy must be maintained for the model to be acceptable (Gordon, 1985).

A model mainly used for: -

- Simulation
- Prediction/Forecasting
- Designing/performance Evaluation
- Prognostics/Diagnostics
- Control System Design

A mathematical model can represent simple or complicated systems. A simple example of a mathematical model is an equation representing a certain process. A Manning's equation (2.1) is a hydraulic model used in an open channel to calculate flow depth. Rational equation (2.2) is another example that is used in small watersheds to calculate the runoff exposed to storm rainfall.

$$Q = (1/n).A^{\circ}.R^{2/3} \cdot S^{2/3} \qquad (2.1)$$

Where **Q,** represents river flow ($m^3/s$), $\boldsymbol{A}$°,the cross-sectional area of the channel ($m^2$), **R**, hydraulics radius (m), **S**, the hydraulics gradient (unitless) and **n**, the roughness coefficient (unitless).

$$Q = \left(\frac{1}{360}\right) C.I.A \qquad (2.2)$$

Where **Q**, represents the discharge from catchment ($m^3/s$), **C**, coefficient of runoff (unitless), **I**, the intensity of rainfall (mm/hr) and **A**, the catchment area ($m^2$).

Complicated mathematical models are those models that require large computer storage capabilities and advanced mathematics and programming. Compared to simpler models, these models accurately and precisely depict physical phenomena. They have been and continue to be employed in a variety of tasks ranging from real-time flood event prediction to the design of policies and buildings for mitigating extreme hydrologic events (e.g., floods and droughts). These hydrologic models must be calibrated on a regular basis in order to be effective in solving such current problems (Gupta et al., 2003).

The introduction of the unit hydrograph concept by Sherman in 1932 and the development of infiltration theory by Horton in 1933 marked the beginning of the mathematical modeling of watershed hydrology. The 1960s witnessed the digital revolution that made the integration of different components of the hydrological cycle and the simulation of almost the entire watershed hydrology possible. Since then, the power of the computer has grown exponentially, and watershed hydrology has advanced at an extraordinary rate.

Figure 2.1 is a schematic representation of the mathematical modeling process. The modeling process begins with the characterization of the problem and continues with the building of a simplified and idealized version of the problem through the identification of critical model components and the formulation of hypotheses. The problem is then translated into a mathematical model composed of mathematical phrase variables and defining the variables' interactions. The problem is then evaluated and solved mathematically to obtain the desired results. The results are more transparent when viewed through the lens of a simplified real-world situation. Finally, the solution developed for the simplified version of the problem was verified (sen Zeytun et al., 2016).

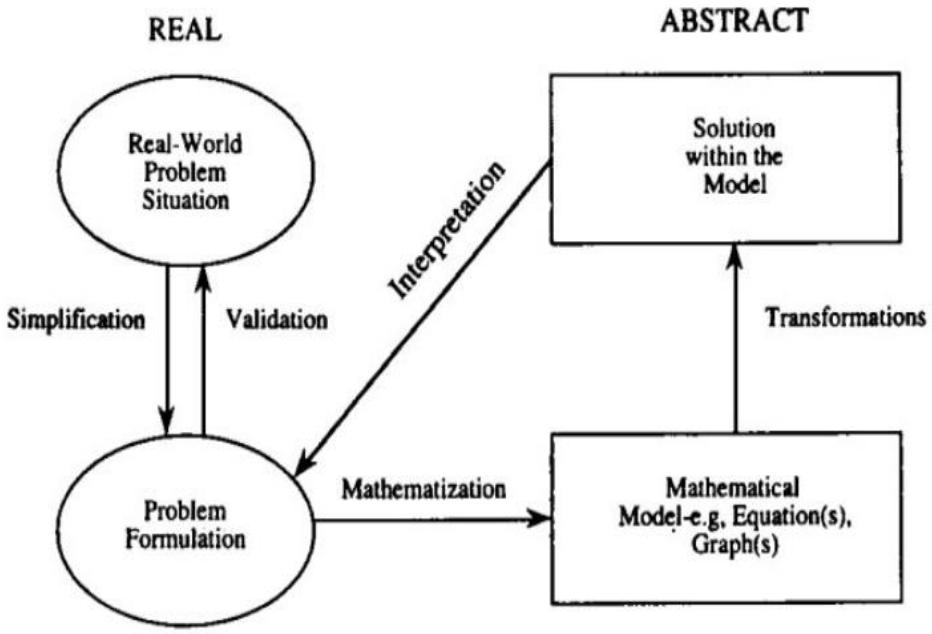


**Figure 2.1.** *Process of mathematical modeling (NCTM, 1989).*

## 2.2. Classification of Mathematical Models

Mathematical models can be divided into two main categories: stochastic and deterministic models. The primary distinction between these two types is that stochastic models are based on statistics and probability and are more concerned with predictions, whereas deterministic models are used to make forecasts. The prediction relates to a set of simulated hydrographs used for engineering design purposes. On the other hand, forecasts refer to simulated hydrographs of certain future events that will be used to make discretionary decisions(Öner, 1997).

In deterministic models like Manning's and rational equations, outcomes are exactly predicted by known correlations between states and events, eliminating the possibility of random variation. There are two types of deterministic mathematical models based on spatial representations: lumped and distributed. Specific catchments are treated as a single element in dimensionless space in the lumped model. However, the distributed model partitions each catchment into smaller parts based on its area size. These models can be either steady-flow or unstable-flow based on the flow rate's relationship to time.

Hydrologic modeling based on events is concerned with the way a basin reacts to its rainfall history (e.g., surface runoff quantity, peak, peak time). On the other hand, continuous hydrologic modeling combines hydrologic processes and phenomena across a long time period in both wet and dry conditions (Steinman et al., 2009). Figure 2.2 summarizes the main categories of mathematical models used in hydrology.

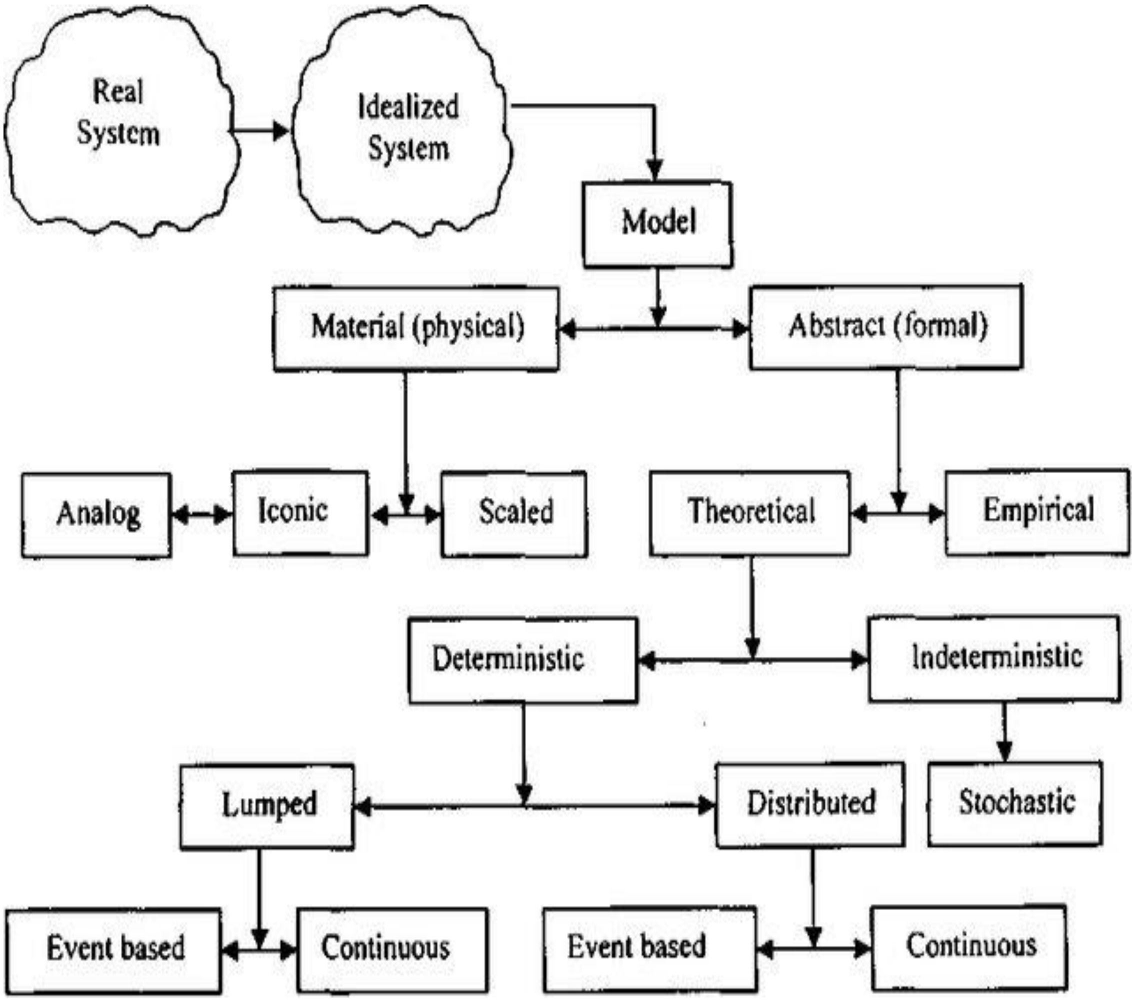


**Figure 2.2.** *Classification of hydrologic models (chow et al,1988)*

## 2.3. Urban Storm Management Model

Urban Stormwater modeling is basically mathematical modeling of stormwater in urban areas to enable designers to analyze and explore innovative stormwater design options and efficiently manage project outputs. Rapid urbanization has numerous undesirable effects on the hydrological cycle by increasing areas imperviousness to stormwater runoff and worsening water quality.

The earliest computational models capable of simulating stormwater quality and quantity were developed primarily by US government agencies, such as the USEPA, in the early 1970s (Zoppou, 2001). Numerous urban watershed models have been produced and discussed in the literature since that time. These models frequently used for planning, designing, flow predicting and screening purpose.

The two fundamental components of any urban storm water model are rainfall-runoff modeling and transport modeling. The link between these components is illustrated in Figure 2.3.

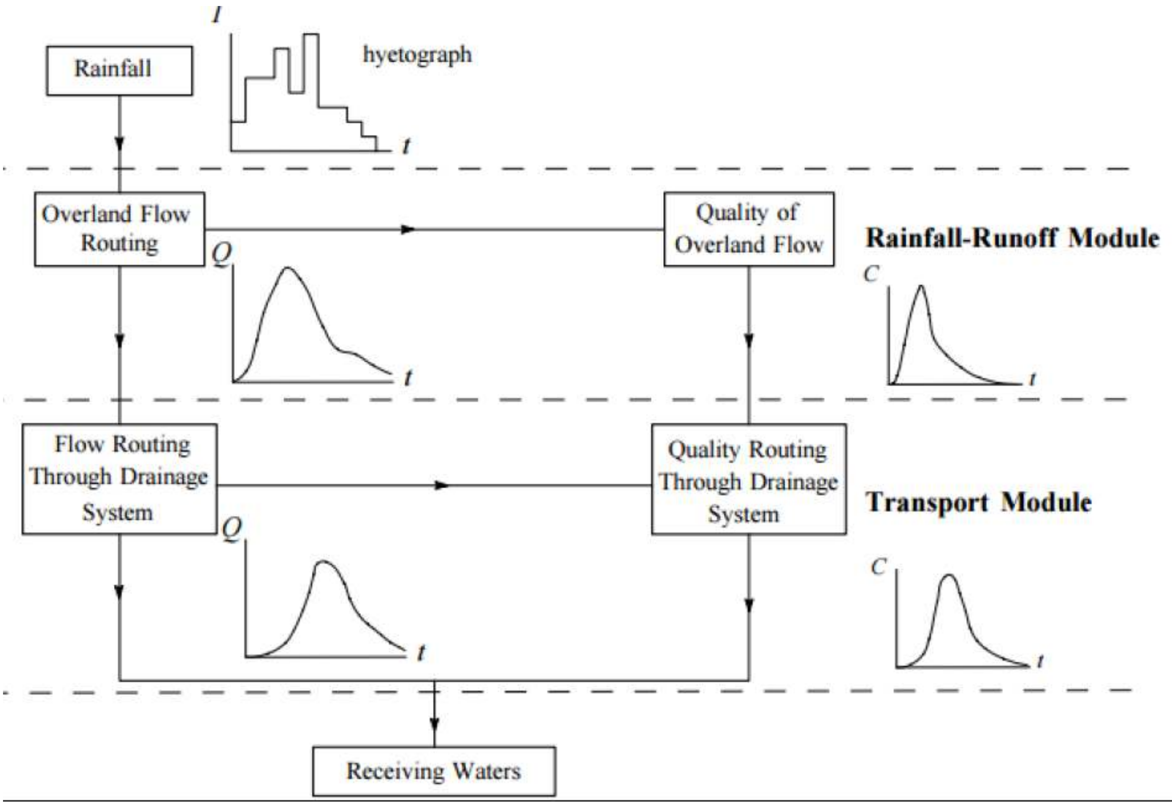


**Figure 2.3.** *A summary of the processes included into a storm water model* (Zoppou, 2001).

There are numerous software packages developed by academic institutions, engineering consultants, regulatory agencies, and government departments that enable the modeling and simulation of water quality and quantity in urban areas. Among them are programs like MOUSE for urban drainage and sewers; Info Works River Simulation (Info Work RS), which simulates a river; Info Works River Simulation; (HSPF), which simulates hydrologic processes; (QQS), which simulates water quality and quantity; (DR3M), which is a rainfall-runoff model; and (XPSWMM), which is a program for managing storm water. (Haris et al., 2016).

Most of these models are 1-D models and are based on the principle of mass, energy, and momentum conservation. Some models are event-based models and others are of continuous simulation type (Nanduri et al., 2018). The summary of comparison between these urban flood models is given in Table 2.1.

***Table 2.1.*** *Comparison of the attributes of Urban Floods*

| **Attributes** | **DR3M** | **HSPF** | **STORM** | **SWMM** |
|---|---|---|---|---|
| Funding agency | USGS | EPA | HEC | EPA |
| Type of Simulation (Event-based/Continuous) | *Both* | *Both* | *Continuous* | *Both* |
| No of pollutants | *4* | *10* | *6* | *10* |
| Analyses of rainfall/runoff | *Yes* | *Yes* | *Yes* | *Yes* |
| Flow routing in the sewer system | *Yes* | *Yes* | *No* | *Yes* |
| Full, Dynamic routing equation | *No* | *No* | *No* | *Yes* |
| Surcharge | *Yes* | *No* | *No* | *Yes* |
| Regulators, overflow, structures such as weirs, | *No* | *No* | *Yes* | *Yes* |
| Storage analysis | *Yes* | *Yes* | *Yes* | *Yes* |
| Treatment analysis | *Yes* | *Yes* | *Yes* | *Yes* |
| Complexity | *Medium* | *High* | *Low* | *High* |
| Data requirement | *Medium* | *High* | *Low* | *High* |

## 2.4. The EPA SWMM

### 2.4.1. Overview

EPA SWMM is a widely used urban flood modeling software that policymakers use to plan and develop adequate urban stormwater drainage systems. It is a stormwater management model that was developed in 1971 by the National Risk Management Research Laboratory of the US Environmental Protection Agency. It is a distributed, dynamic rainfall-runoff simulation model that is mostly used in urban areas to simulate the quantity and quality of event-based or continuous runoff.

SWMM's runoff component is composed of a network of sub-basin locations that receive precipitation and create runoff and pollutant loads. The SWMM's routing section transports this flow through a network of pipes, pumps, conduits, regulators, and storage/treatment devices. SWMM continuously analyzes the quantity and quality of runoff produced in each sub-basin, as well as the flow rate, flow depth, and quality of water flowing through each pipe and channel over a multiple-time step simulation period (Huber & Barnwell, 1988)

As a low-impact development (LID) control, SWMM allows engineers and planners to express combinations of green infrastructure techniques. Additionally, several of these approaches can have significant pollution reduction advantages.

SWMM's typical applications include the following:

- Drainage system component design and sizing for flood control.
- Developing control measures to keep combined sewer overflows to a minimum.
- Conducted a study on how inflow and infiltration affect sanitary sewer overflows.
- Controlling site runoff using low LID controls such as green infrastructure initiatives.
- Estimating the dimensions of detention facilities for flood management and water quality preservation.
- Evaluating the effectiveness of best management techniques and low-impact development (LID) in lowering pollutant loadings during wet weather.

SWMM, as illustrated in Figure 2.4, has a variety of physical elements that are utilized to simulate a drainage system. Some are hydraulic in character, while others are hydrologic.

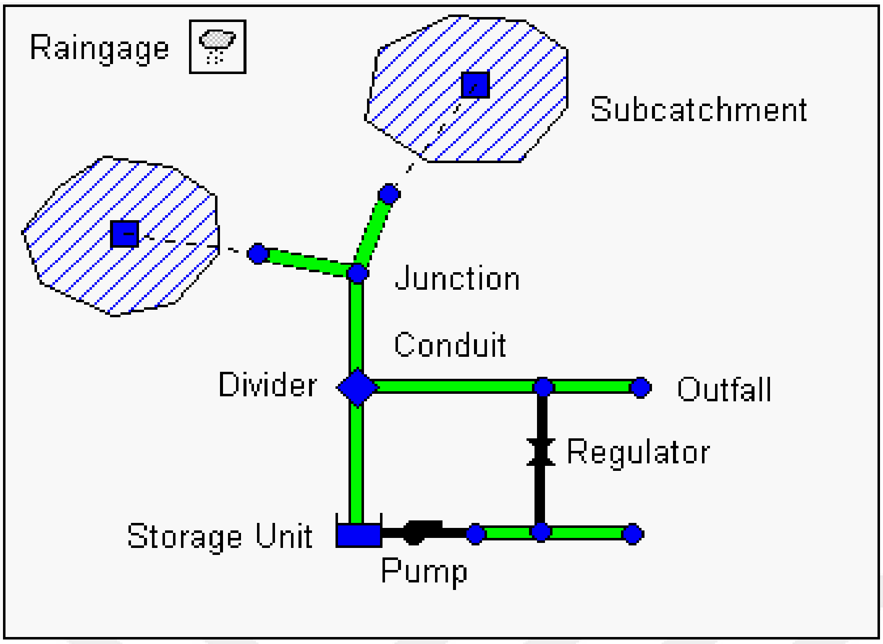


**Figure 2.4.** *Physical objects that operate as a representation of a drainage system* (Rossman, 2015).

***Table 2.2.*** *Summary of Hydraulic and hydrologic elements in SWMM* (Rossman, 2015).

| **Symbol** | **Physical object** | | **Function** |
|---|---|---|---|
|  | Raingage | - | Used to provide precipitation data for a research area's one or more subcatchment zones. |
|  | Subcatchment | - | Used to direct surface runoff to a single point of discharge. |
|  | Junction | - | Used to combine flows from upstream reaches and subbasins |
|  | Outfall | - | Used to represent the outlet of the physical watershed. |
|  | Flow divider | - | used to direct inflows to a given conduit in a predetermined way |
|  | Storage unit | - | used to provide storage volume |
|  | Conduit | - | used in the basin model to transport (route) water from one node to another |
|  | Pump link | - | is a link used to send water to high elevations |

### 2.4.2. Governing equation

SWMM, as previously stated, is a distributed, public, dynamic rainfall-runoff simulation model mainly used for event-based and continuous modeling of urban runoff quantity and quality. As illustrated in Figure 4.1, SWMM defines a subcatchment as a rectangular surface with a consistent slope (S) and width (W) that flows into a single outlet channel. The terrestrial flow is generated by simulating the sub-basin as a non-linear reservoir, as seen in Figure 4.2.

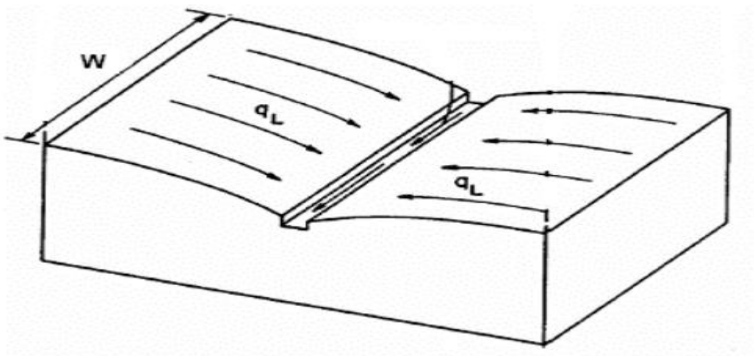


**Figure 2.5.** *Idealized sub-catchment representation*

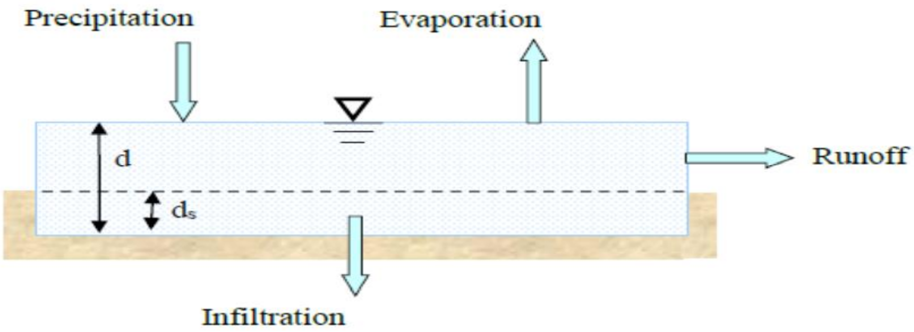


**Figure 2.6.** *A nonlinear subcatchment's reservoir model*

EPA SWMM is a mathematical model, which means it has governing equations to describe how the unknown variable values change depending on the change in one or more known variables. Conservation of energy, conservation of mass, conservation of momentum, and saint-Venant flow equations are some examples of governing equations in mathematical models. There are governing equations in SWMM that apply to both hydrological and hydraulic modeling.

Equation 4.1 mentions the governing equation for the hydrology part of SWMM, which is an overland flow that comes from modeling the sub-catchment as a nonlinear reservoir.

$$\frac{\partial d}{\partial t} = i - e - f - q \qquad (4.1)$$

Where, i = rainfall + snowmelt rate (ft/s)

e = rate of surface evaporation (ft/s)

f = rate of infiltration (ft/s)

q = runoff rate (ft/s)

SWMM's hydraulic flow routing is governed by mass and momentum conservation equations for gradually changing, unstable free surface flow. This equation called the saint venant flow equations.

- ✓ Contunity

$$\frac{\partial A}{\partial t} + \frac{\partial Q}{\partial x} = 0 \qquad (4.2)$$

Where, x = distance (ft) A = cross-sectional area of the flow (ft^2)

t = time (sec) Q =flow rate (cfc)

- ✓ Momentum

$$\frac{\partial Q}{\partial t} + \frac{\partial (Q^2/A)}{\partial x} + gA\frac{\partial H}{\partial x} + gAS_f = 0 \qquad (4.3)$$

Where, H = water's hydraulic head in the conduit (Z + Y) (ft)

Z= is the inverted elevation of the conduit (ft)

Y = Water depth in the conduit (ft)

Sf = friction coefficient (head loss per unit length)

g = gravitational acceleration (ft/sec2)

## 3. RESEARCH METHODOLOGY

### 3.1. Research Location

Boğaziçi Neighborhood is located in the Mamak district of Ankara, the capital city of Turkey. It is located at an average altitude of 1021 m above sea level, and the total drainage area is approximately. The Boğaziçi Neighborhood is mainly characterized by high-sloping areas, with an average slope of 12%. The highest altitude in the study area is 1077 meters, and the lowest point is 924 meters. The outfall of the study area is discharged into the Hatip Stream. An underground pipeline diverts rain and sewage. Because of its mountainous structure, this region is constantly flooded throughout the rainy season. This research area is a good representation of a flood simulation.

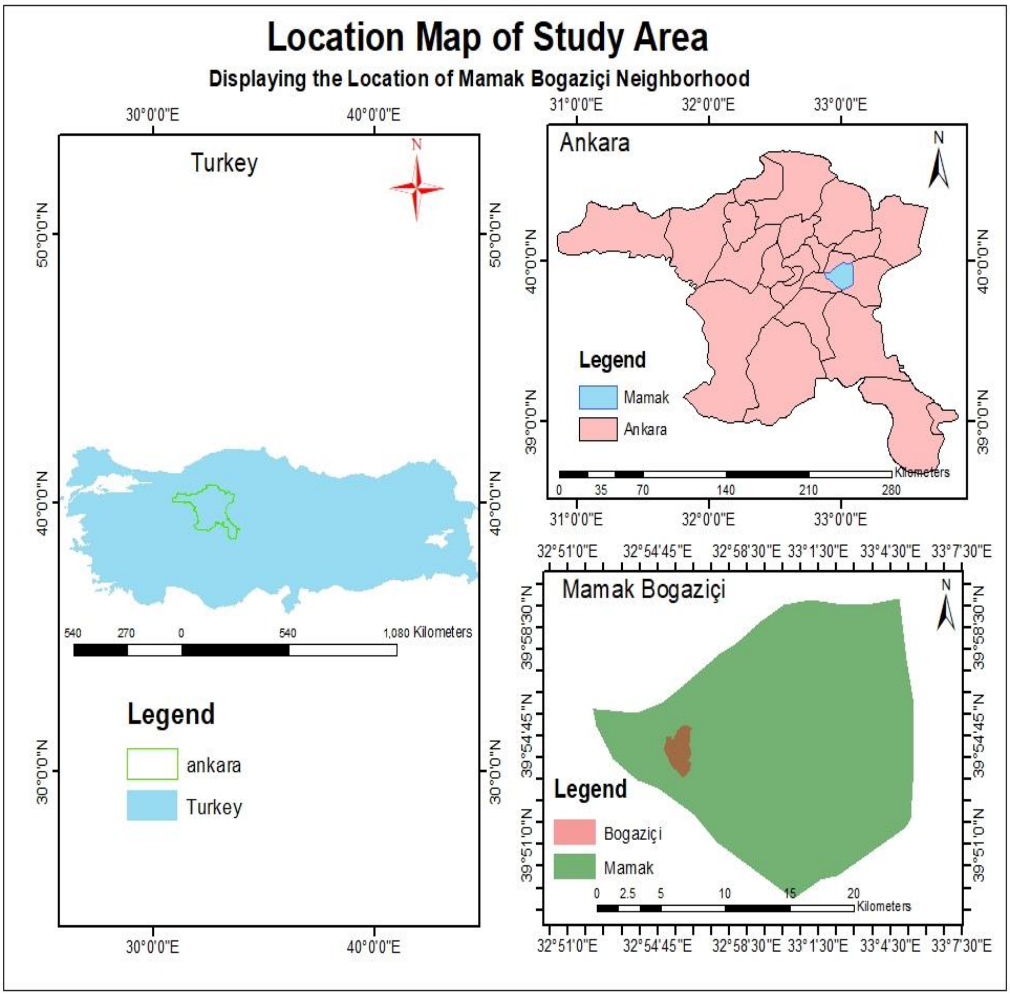


**Figure 3.1.** *Location of study area Mamak Boğaziçi Neighborhood (by ARC GIS)*

This area was chosen as the study area as it is subject to additional flooding, usually during the rainy seasons. There has also been significant infrastructure development in the recent past. In addition, the overflow can be directed to the Hatip Stream, which is not far from the outlet of the area.

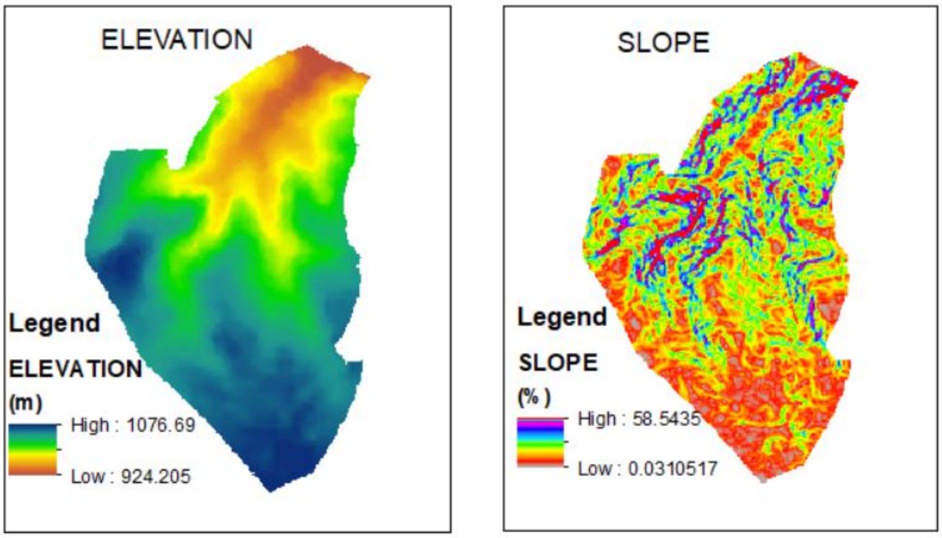


**Figure 3.2.** *Slope and Digital Elevation Map (DEM) of study area (by ARC GIS)*


**Figure 3.3.** *Study area image on Google Map (by Google Earth pro)*

## 3.2. Model Process

Flood simulations built on SWMM include a collection of procedures that simulate runoff in specific fields. More precisely, it necessitates a completely defined project area. The data needed to compute the simulation for this defined project area should be organized in a way that the SWMM can understand. The model must then be calibrated, and the parameters changed appropriately to accurately reflect the drainage features of the research area. In the end, a model that utilizes SWMM for flood computation has been obtained. This model could be very useful for the study area. It could be used for more drainage analysis and managerial decisions in the project area (Wang et al., 2019).

To perform this SWMM-based flood modeling, there are five major phases, as illustrated in Figure 3.4: prophase preparation, data processing, parameter setting, model simulation, and model validation.

The Prophase preparation stage consists of resource collection and situation awareness. Resources include all kinds of required data and information for the modeling process. Situation awareness refers to the knowledge of the condition of the real situation through a broad view and perception. It's important to know what the project area is like and how to work with the data at this point (Badham et al., 2019).

The spatial data processing phase includes processes such as rain gauge establishment, sub-catchment division, and drainage system description, which help to prepare a suitable data entry for the model that can replicate the physical properties of the research area. Common sub-watershed partitioning can be drawn either manually, with GIS techniques, or by combining both (Lv et al., 2017). The basis and guidelines for dividing a catchment may similarly differ, as the effects of land and construction are handled in different ways in various circumstances (Sun et al., 2014).

In the property parameter setting stage, further parameters are determined and allocated to the separate outcomes from the previous stage of spatial data processing in order to accurately describe the research area. This stage involves setting the properties of rain gauges and sub-catchments. The parameters we set may be calculable parameters, measurable parameters, or calibrated parameters (Wang et al., 2019). Those parameters linked with the characteristics of the physical elements in the research area, and which can be directly taken from already quantified data are measured parameters. This includes parameters like pipeline size or bore hole depth. Calculable parameters are parameters that can be computed through GIS techniques or geometric approaches, such as the area catchment, the mean slope, and the impervious area percentage (Rana & Suryanarayana, 2020). These parameters, such as depression storage volume of pervious and impervious areas and manning coefficient, which are established on prior experience and are regulated properly, are calibrated parameters (Zhang et al., 2022).

Before the model verfication phase, the data needed by the model should be converted to the desired format, simulation options should be set for the model, and SWMM should be run. All these processes are included in the model simulation phase. The first activity at this stage is to change the feature parameters of drainage system, rain gauges, and sub-basin and descriptions of spatial geometric into the input data setup operated by SWMM (@inp format). SWMM execution and general troubleshooting strategies are then applied to ensure the model is ready to run (Zhang et al., 2022).

The model verification stage is the final stage of the model process in SWMM for flood modeling. This step evaluates the accuracy of the produced flood model and determines whether it requires further development to ensure the model's practicability and consistency. The model verification stage is concerned with managing the simulation's output. By comparing them to actual conditions, one can ascertain whether the flood simulation produced the expected result (Rosa et al., 2015).This stage includes references to the wide range of runoff coefficients provided by the drainage system's design, comparsion of the distribution of flood-prone points for each rainfall event or return period, and explanations of the relationship between outlet discharge and precipitation sequence. These standards and approaches are quite beneficial for verifying a model (Yu et al., 2014).

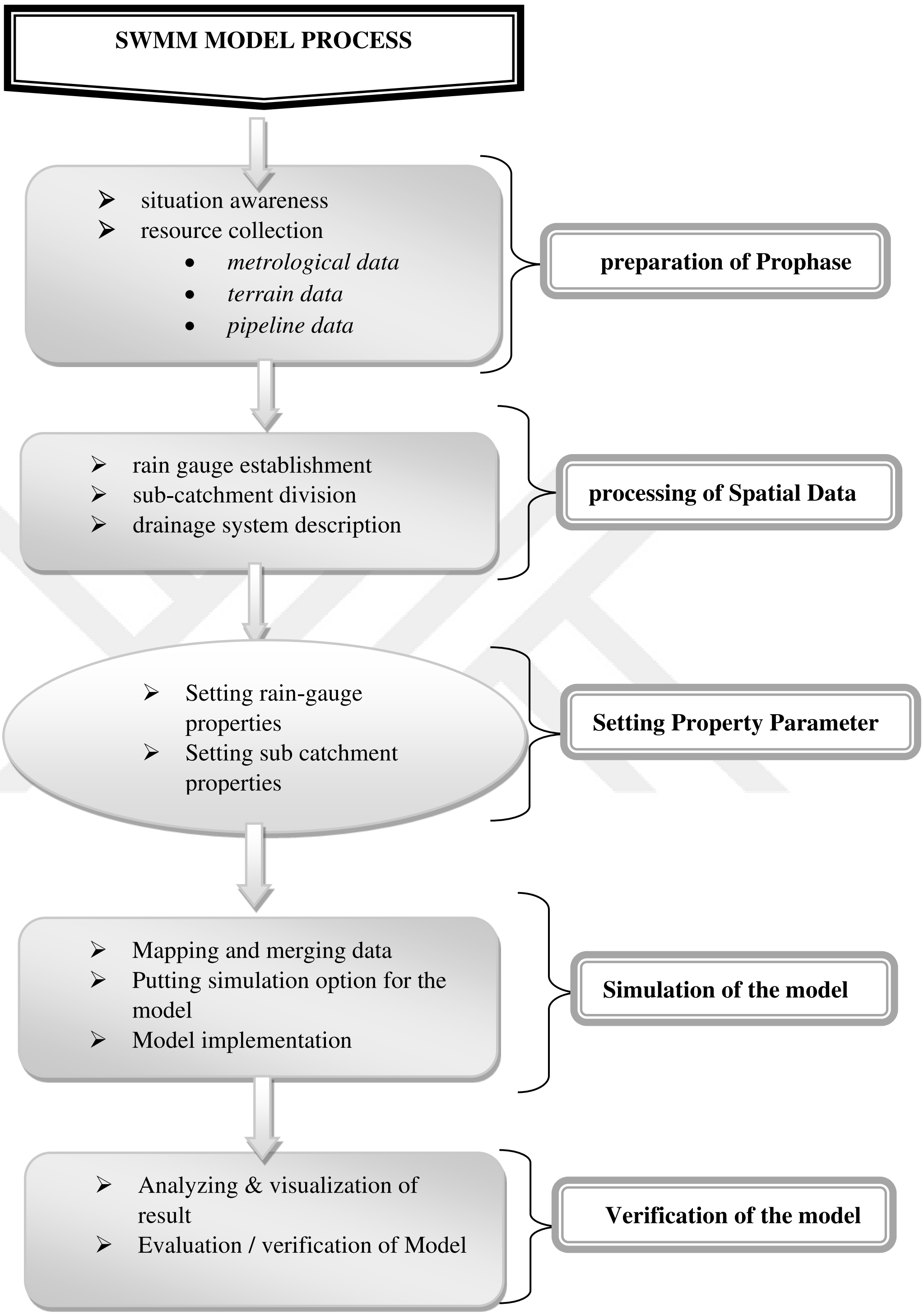


**Figure 3.4.** *The flow chart of the simulation model development in EPA SWMM.*

## 3.3. Data Collection

Data collection is a vital step in this project since accurate and reliable data influences the quality of the SWMM model. This section discusses the types of data that are needed to build, calibrate, and validate a SWMM model. It also describes the methods used in collecting this data. The data required to model an urban flood scenario using SWMM comprises both hydrological and hydraulic data. Hydrological data, including subcatchment characteristics, single-event rainfall data, and rainfall intensity–duration–frequency curves for various return periods. Hydraulic data includes node and pipe parameters. In the modeling procedure, data for single events and IDF curves of rainfall were gathered from the Turkish state metrological agency.

Subcatchment features and pipe information are the most important data used for model building in SWMM. This includes information on the area, slope, percentage, and topography of sub-basins, as well as information on channels and their size. Most of the subcatchment specification data is obtained using GIS-based software such as ARC-GIS and Google Earth. Data on pipe properties (depth, length, & manning roughness depend on material made) and terrain properties were obtained from the Ankara Water and Sewerage Administration General Directorate (ASKI).

**Table 3.1.** *Data relating to the study area*

| Data | Format | Explanation | Source |
|---|---|---|---|
| Network data | Polyline shapefile (pipeline) | Diameter, length, material made | *ASKI** |
| Terrain data | Polyline, point shapefile, DEM | Contour lines DEM 30m × 30m | ASKI |
| Precipitation data | XLS | hourly total precipitation (mm) | Turkish state metrological service. |
| IDF curve | Image/XLS | Designed storm | Turkish state metrological service. |

* Ankara water and sewerage administration general directorate.

### 3.4. Model Evaluation and Efficiency Criteria

Model evaluation is the process of assessing models using statistical measures to determine the accuracy and reliability of predictions when compared to observed data. Evaluations of hydraulic behavior and performance are often done and reported by comparing simulated and observed data. Goodness of fit measurements can be used to assess model predictions. These measurements are too sensitive to extreme values (outliers) and underly sensitive to additive and proportional variations between model predictions and observed values. The majority of them are correlation-based measurements. The efficiency criteria include the Nash and Sutcliffe efficiency, coefficient of determination, and index of agreement. RMSE (Root-Mean Square Error), MAE (Mean Absolute Error), BIAS, and Volume Error are among the error detection criteria.

The Nash and Sutcliffe Efficiency (NSE) is a measure of efficiency that connects the model's goodness-of-fit to the variance of measured data. NSE can vary from 0 to 1, with 1 indicating a perfect match between observed and simulated discharges.

$$NSE = 1 - \left[\frac{\sum_{i=1}^{n}(Q_i^g - Q_i^m)^2}{\sum_{i=1}^{n}(Q_i^g - Q^o)^2}\right] \qquad (5.1)$$

Where $Q_0$= Discharge measured

$Q_s$= Discharge simulated

$\overline{Q}_0$= average of calculated flow

An index of agreement (d) is a standardized measure of model prediction error ranging from 0 to 1. The index of agreement is the ratio of mean square error to potential error. A score of 1 shows a perfect match, whereas a value of 0 indicates no agreement at all. The index of agreement may identify additive and proportional differences in observed and simulated means and variances; however, due to squared differences, d is extremely sensitive to extreme values (Willmott et al., 2012)

$$d = 1 - \frac{\sum_{i=1}^{n}(O_i - P_i)^2}{\sum_{i=1}^{n}(|P_i - \bar{O}| + |O_i - \bar{O}|)^2} \quad , \quad 0 \leq d \leq 1 \qquad (5.2)$$

where $O_i$ is the observation value and $P_i$ is the forecast value and O-bar is the average observation values and P-bar is the average forecast values.

The R-squared correlation coefficient is a critical statistical measure that indicates the proportion of the difference or variance in statistical terms for a dependent variable that can be explained by an independent variable or variables in a regression model. In a simple terms, R-squared correlation indicates the degree to which data fits the regression model or the modeled data fits the observed data. The determination coefficient, R2, is comparable to the correlation coefficient, R. Correlation coefficients indicate the strength of a linear link between two variables. R-Squared is the correlation coefficient's square. R-squared is calculated by first calculating Pearson correlation and then squaring it (AgriMetSoft, 2019).

$$\mathbf{r} = \frac{\mathbf{n}(\sum \mathbf{xy}) - (\sum \mathbf{x})(\sum \mathbf{y})}{\sqrt{[\mathbf{n}\sum \mathbf{x}^2 - (\sum \mathbf{x})^2][\mathbf{n}\sum \mathbf{y}^2 - (\sum \mathbf{y})^2]}} \qquad 5.3$$

Where r = Pearson correlation

n = number in the given dataset

x = observed data

y = modeled data

# 4. MODELING AND SIMULATION

## 4.1. Base Model Development

When we look at the distribution of flood disasters in Turkey over a long period of time, we can see that flood disasters are most common in large settlements with high population density, such as Ankara, Balıkesir, Izmir, and Antalya. In other words, when we group the floods in our country according to the places where they occur, it is seen that the most common floods are urban floods (Ceylan et al., 2015).

In this research, the storm water simulation package EPA SWMM has been used for urban flood modelling of the Boğaziçi neighborhood in Mamak district of Ankara. In May 2018, torrential rain that lasted for about 12 minutes caused a disaster. Floodwaters dragged dozens of vehicles in front of them, 6 people were injured in the flood, more than 20 workplaces and more than 150 vehicles were damaged. This flood disaster mainly occurred in Neşet Ertaş Street of Mamak Boğaziçi neighborhood(Goren & Goksu, 2018).

**Figure 4.1.** *Flooding in Neşet Ertaş Street and around the outfall of the study area (May 2018)*

## 4.2. Modeling Using EPA SWMM

### 4.2.1. Modeling and simulating the study area in SWMM

The following steps should be carried out to model study area using EPA SWMM:

- Set the default parameters and object properties to be used.
- Describe the physical elements of the research area.
- Changing the attributes of the objects that make up the system Editing object
- Choose an option for analysis
- Running the simulation
- Observe the result of simulation

#### *4.2.1.1. Setting default option*

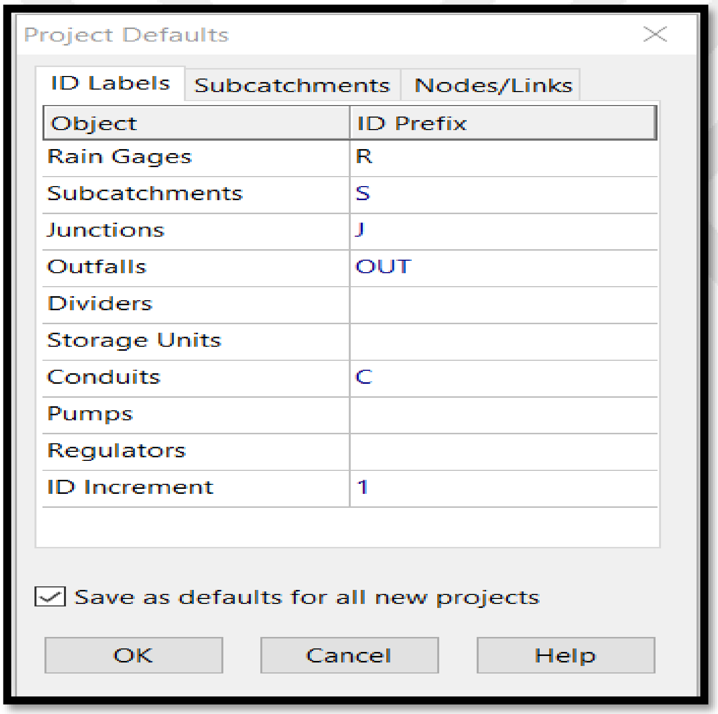


***Figure 4.2.*** *ID labels default for the study area*

The first step in this project is to define a default set of parameters in order to avoid errors and repetition. Defaults for ID labels, sub-catchments, and node properties are the main categories of default in EPA SWMM. The default ID labels used to identify junctions and conduits in this project are shown in Figure 4.4. Since sub-catchments and nodes have different properties, their defaults were not set to them.

### *4.2.1.2. Description of physical components*

The next step is to put an image as a backdrop behind a project's study area map to simplify the arrangement of drainage-system objects. For this project, the backdrop image comes from CAD and GIS drawings of the study area, and all sub-basins are arranged on the image for easy drawing of the sub-basin in SWMM.

As shown in Figure 4.5, The study area is sub divided in to 28 sub-catchments(S), 21 junctions(J) and 21 conduits(C). The sub-catchment division performed by manual drawing depend on the topography of study area. The sub-catchment boundaries were determined by combining sub-areas whose possible overland flow paths share a common direction and drain to the same collection channel.

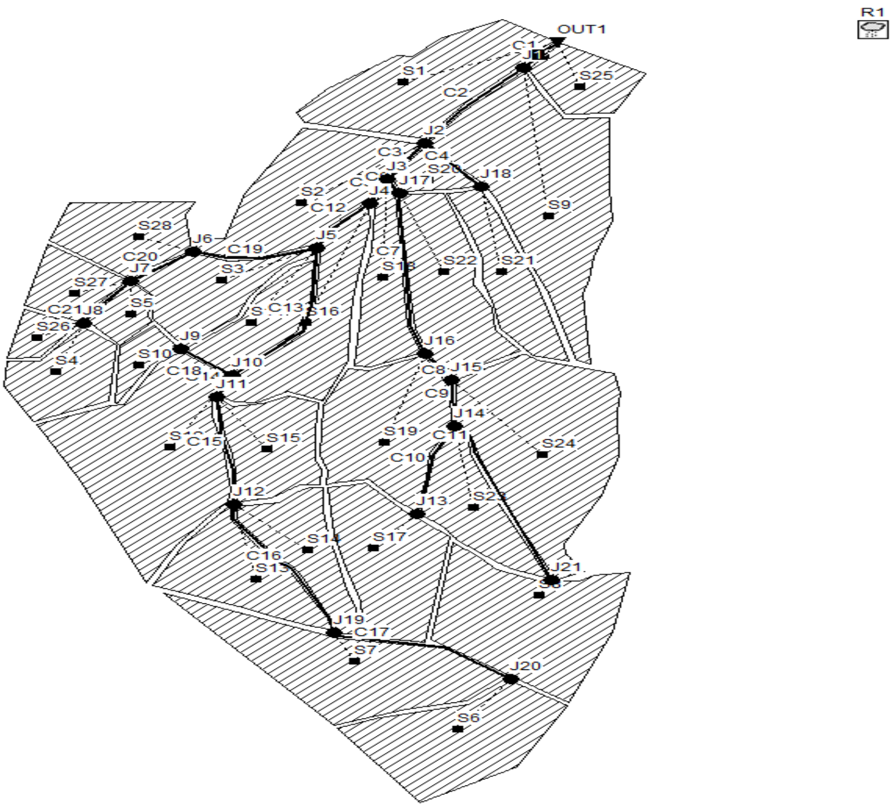


**Figure 4.3.** *SWMM description of the study area map's physical components*

### *4.2.1.3. Editing Object Properties*

Prior to altering an object that appears in this research area, the unit system used to express the object's characteristics changes in accordance with the flowrate unit. In this research, the SI metric units were used to describe the attributes of objects. Appendix A.1 has the units for all properties.

Geometric properties (area, width, slope, and imperviousness), roughness coefficients, depression storages, and infiltration parameters are assigned to each subcatchment. Sub-catchment's area, width, and slope are easily estimated using ARC-GIS.

In SWMM, the imperviousness parameter is the efficient or directly connected impermeable area, which is always smaller than the overall imperviousness. Effective impervious area is defined as impervious area that drains directly into a stormwater sewer network (SWMM app manual). In this study, the imperviousness property of a sub-catchment was obtained based on the land use categories listed in Table 4.1. The imperviousness (I) is then calculated as the area weighted average of the runoff coefficients for all land uses inside the sub-catchment, with I = (CjAj)/A, where A is the sub-total catchment's area and C is the runoff coefficient. The other parameters were chosen in accordance with the typical values indicated in the literature (Huber & Barnwell, 1988; Ponce & Hawkins, 1996; Rossman, 2010).

**Table 4.1.** *Land use categories in the study area (Huber & Barnwell, 1988)*

| ID | Land use | Runoff coefficient (C) |
|---|---|---|
| M | Medium density | 0.65 |
| L | Low density | 0.45 |
| DL | Duplex | 0.70 |
| S | Apartment, high density | 0.70 |
| RT | Commercial | 0.95 |
| P | Natural (park) | 0 |

Sub-catchment properties are the most important properties in modeling SWMM. Because it is the one that determines the model the most and contains more parameters than the other SWMM elements. The summary for geometrical sub-catchment properties is mentioned in Table 4.2. The value for depth of depression storage on pervious and impervious area ( Dstore-per and Dstore-imperve ) for all subcatchments taken as 0.05 mm defaultly.

**Table 4.2.** *Subcatchment properties of the study area*

| Sub- ID | Area(ha) | Width (m) | Outlet | Impervi- (%) | N-perv | N-imperv | Slope (%) |
|---|---|---|---|---|---|---|---|
| **S1** | 16.30 | 498 | Out-1 | 53.0 | 0.1 | 0.012 | 15.5 |
| **S2** | 16.90 | 348 | J2 | 45.0 | 0.1 | 0.012 | 19.4 |
| **S3** | 9.58 | 259 | J5 | 70.0 | 0.1 | 0.012 | 21.7 |
| **S4** | 7.91 | 253 | J8 | 63.4 | 0.1 | 0.012 | 2.9 |
| **S5** | 2.75 | 136 | J7 | 61.1 | 0.1 | 0.012 | 14.9 |
| **S6** | 16.40 | 558 | J20 | 58.2 | 0.1 | 0.012 | 2.2 |
| **S7** | 19.30 | 643 | J19 | 56.4 | 0.1 | 0.012 | 2.8 |
| **S8** | 21.00 | 393 | J21 | 55.0 | 0.1 | 0.012 | 3.2 |
| **S9** | 28.40 | 448 | J1 | 70.0 | 0.1 | 0.012 | 17.6 |
| **S10** | 2.61 | 111 | J9 | 70.0 | 0.1 | 0.012 | 7.2 |
| **S11** | 7.43 | 354 | J5 | 45.0 | 0.1 | 0.012 | 25.8 |
| **S12** | 28.10 | 468 | J10 | 75.0 | 0.1 | 0.012 | 11.1 |
| **S13** | 11.10 | 287 | J12 | 95.0 | 0.1 | 0.012 | 4.7 |
| **S14** | 8.54 | 253 | J12 | 75.0 | 0.1 | 0.012 | 10.3 |
| **S15** | 9.64 | 315 | J11 | 75.0 | 0.1 | 0.012 | 13.5 |
| **S16** | 12.30 | 600 | J4 | 66.0 | 0.1 | 0.012 | 24.0 |
| **S17** | 14.90 | 363 | J13 | 70.0 | 0.1 | 0.012 | 7.2 |
| **S18** | 8.41 | 262 | J3 | 45.0 | 0.1 | 0.012 | 19.6 |
| **S19** | 16.70 | 326 | J16 | 70.0 | 0.1 | 0.012 | 11.9 |
| **S20** | 2.41 | 103 | J2 | 70.0 | 0.1 | 0.012 | 15.4 |
| **S21** | 9.20 | 351 | J18 | 75.0 | 0.1 | 0.012 | 18.9 |
| **S22** | 14.20 | 580 | J17 | 45.0 | 0.1 | 0.012 | 19.6 |
| **S23** | 9.32 | 572 | J14 | 75.0 | 0.1 | 0.012 | 9.3 |
| **S24** | 27.60 | 328 | J15 | 57.5 | 0.1 | 0.012 | 13.6 |
| **S25** | 4.13 | 118 | Out-1 | 30.0 | 0.1 | 0.012 | 19.56 |
| **S26** | 2.37 | 158 | J8 | 70.0 | 0.1 | 0.012 | 13.7 |
| **S27** | 4.67 | 227 | J7 | 70.0 | 0.1 | 0.012 | 15.8 |
| **S28** | 9.51 | 352 | J6 | 70.0 | 0.1 | 0.012 | 18.7 |

Apart from sub-catchments, the other hydrological element in this project is rain gages, which are used to define rainfall parameters. SWMM accommodates for rainfall's geographic variability by allowing the user to establish an unlimited number of rain gauge objects, as well as individual data sources and the allocation of each rain gauge to a single SWMM sub catchment object (i.e., land parcel) from which runoff is estimated. Rainfall data is critical for runoff estimation and flood analysis, which are used to build hydraulic structures. Hourly total precipitation data recorded from the Mamak Bayndir Dam rain gauge station (during exceptional occurrences) were utilized to compute rainfall for this research, as indicated in Tables 4.3 and 4.4.

**Table 4.3**. *Hourly total precipitation data for 20th May of 2018*

| Station | Event time (M/D/Y) | Hours | Total Precipitation (mm) |
|---|---|---|---|
| Mamak Bayndir Dam | 05/20/2018 | 13:00 | 0.0 |
| | | 14:00 | 0.4 |
| | | 15:00 | 2.9 |
| | | 16:00 | 2.4 |
| | | 17:00 | 1.8 |
| | | 18:00 | 6.2 |
| | | 19:00 | 0.2 |
| | | 20:00 | 0.2 |

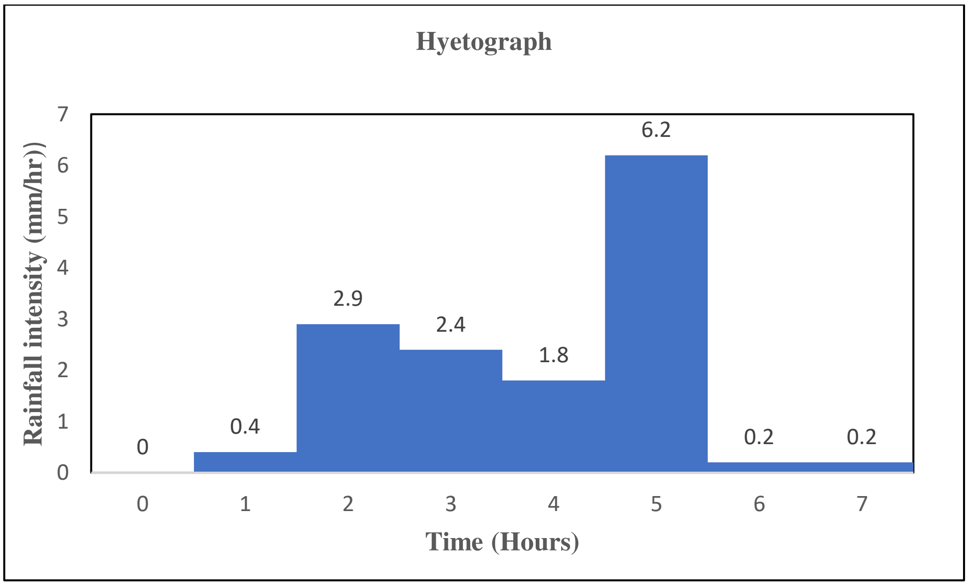


**Figure 4.4.** *Hyetograph of Hourly total precipitation data for 20th May of 2018*

**Table 4.4.** *Hourly total precipitation data for 9th June of 2021*

| Station | Event time (M/D/Y) | Hours | Total Precipitation (mm) |
|---|---|---|---|
| | | 04:00 | 0.0 |
| | | 05:00 | 0.2 |
| | | 06:00 | 0.0 |
| | | 07:00 | 0.0 |
| | | 08:00 | 0.0 |
| Mamak Bayndir Dam | 06/09/2021 | 09:00 | 0.0 |
| | | 10:00 | 0.0 |
| | | 11:00 | 0.0 |
| | | 12:00 | 0.0 |
| | | 13:00 | 4.2 |
| | | 14:00 | 2.0 |
| | | 15:00 | 10.8 |
| | | 16:00 | 0.0 |

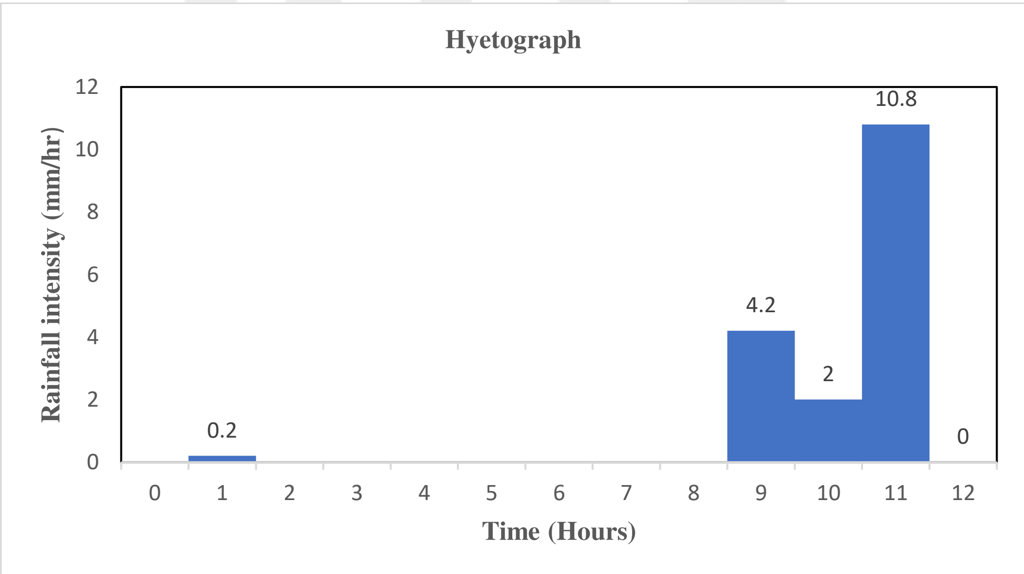


**Figure 4.5.** *Hyetograph of Hourly total precipitation data for 9th June of 2021*

The remaining rainfall data set comprises synthetic design events that simulate storms lasting two, five, ten, fifty, and one hundred years. Each storm is represented by a distinct time series object comprised of cumulative rainfall data collected at one-hour intervals. In the SWMM model, time series of 2, 5 10 ,50 and 100 years are defined. These design storms were created using the Ankara municipal city's intensity-duration-frequency (IDF) curve, as seen in figure 4.8 and in Table 4.5.

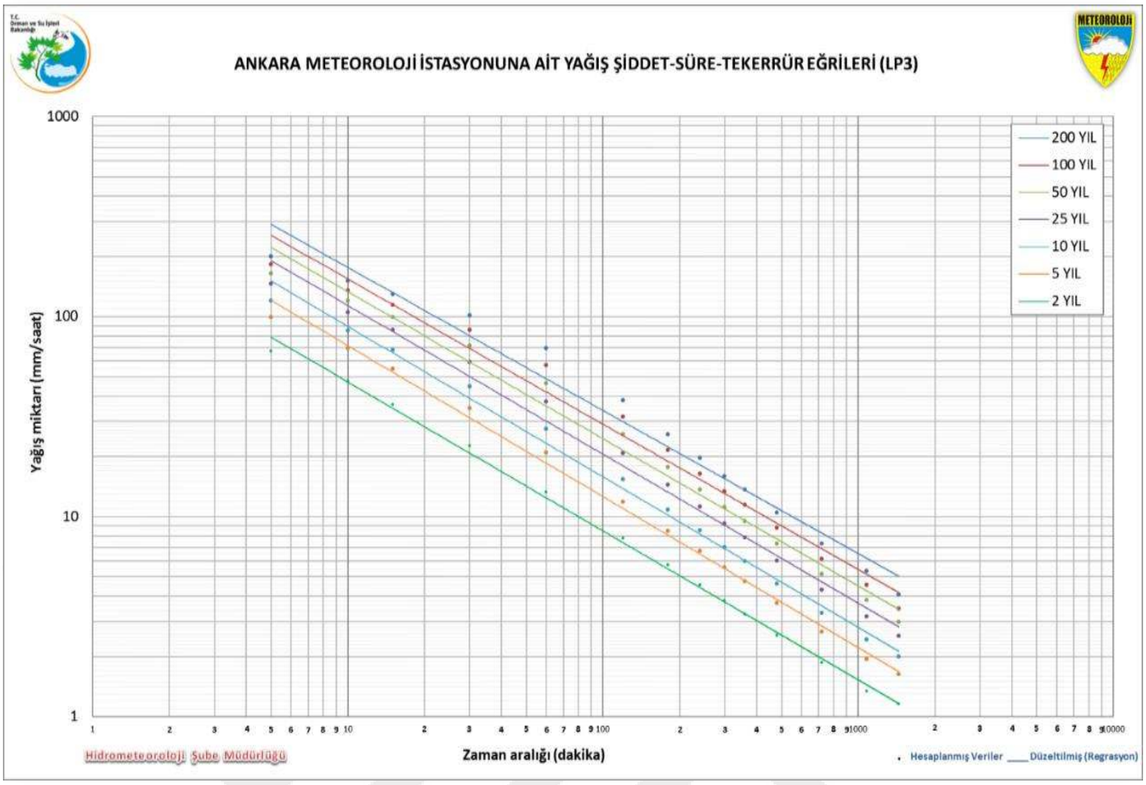


**Figure 4.6.** *IDF curves of Ankara metrology station for different design storms, Vertical axis (intensity -mm/hr.), Horizontal axis (Duration-minutes) source (Turkish state metrological service)*

**Table 4.5.** *Largest rain values observed at Ankara metrology station for different return periods in mm.*

| Return period | MINUTES | | | | HOUR | | | | | | | | | |
|---|---|---|---|---|---|---|---|---|---|---|---|---|---|---|
| | 5 | 10 | 15 | 30 | 1 | 2 | 3 | 4 | 5 | 6 | 8 | 12 | 18 | 24 |
| 2 Year | 5.6 | 7.9 | 9.1 | 11.3 | 13.3 | 15.6 | 17.2 | 18.2 | 18.9 | 19.6 | 20.4 | 22.3 | 24.1 | 27.7 |
| 5 year | 8.3 | 11.6 | 13.7 | 17.4 | 20.9 | 23.7 | 25.5 | 26.9 | 27.8 | 28.5 | 29.5 | 31.8 | 34.9 | 39.2 |
| 10 Year | 10.0 | 14.2 | 17.0 | 22.4 | 27.4 | 30.7 | 32.5 | 34.1 | 35.1 | 35.8 | 36.9 | 39.6 | 43.7 | 48.1 |
| 25 year | 12.1 | 17.5 | 21.4 | 29.6 | 37.5 | 41.5 | 43.4 | 45.0 | 46.1 | 47.1 | 48.3 | 51.5 | 57.1 | 60.8 |
| 50 Year | 13.7 | 20.0 | 24.9 | 35.8 | 46.5 | 51.4 | 53.1 | 54.6 | 55.8 | 57.0 | 58.4 | 62.0 | 68.8 | 71.4 |
| 100 year | 15.2 | 22.5 | 28.5 | 42.8 | 57.0 | 62.9 | 64.3 | 65.6 | 66.9 | 68.5 | 70.0 | 74.0 | 82.1 | 83.1 |
| 200 Year | 16.7 | 25.1 | 32.3 | 50.6 | 69.3 | 76.4 | 77.5 | 78.3 | 79.6 | 81.7 | 83.4 | 87.7 | 96.0 | 97.4 |

Rainwater grills are considered as junctions (nodes) in this project. One of the most important Junction properties is the invert elevation. It is the absolute elevation of the bottom of the junction, and it can be calculated from pipe length and slopes. Table 4.5 shows the summary for the inverted elevation of junctions. In order to prevent backward flow, elevation location should be such that flow from downstream to upstream is prevented. The location of junctions in the study area is illustrated in Figure 4.7. The maximum invert elevation is at Junction 20 (J20), and the minimum is at the outfall of the study area (Table 4.6).

**Table 4.6.** *Invert elevations of junctions and outfall for the study area*

| Nodes | Invert elevation (m) | Nodes | Invert elevation (m) |
|---|---|---|---|
| J1 | 919.36 | J12 | 952.97 |
| J2 | 924.36 | J13 | 954.92 |
| J3 | 926.68 | J14 | 943.61 |
| J4 | 927.87 | J15 | 940.03 |
| J5 | 931.33 | J16 | 938.26 |
| J6 | 934.67 | J17 | 927.89 |
| J7 | 937.61 | J18 | 927.36 |
| J8 | 942.43 | J19 | 992.37 |
| J9 | 981.33 | J20 | 1000.37 |
| J10 | 944.33 | J21 | 957.58 |
| J11 | 945.9 | OUT-1 | 918 |

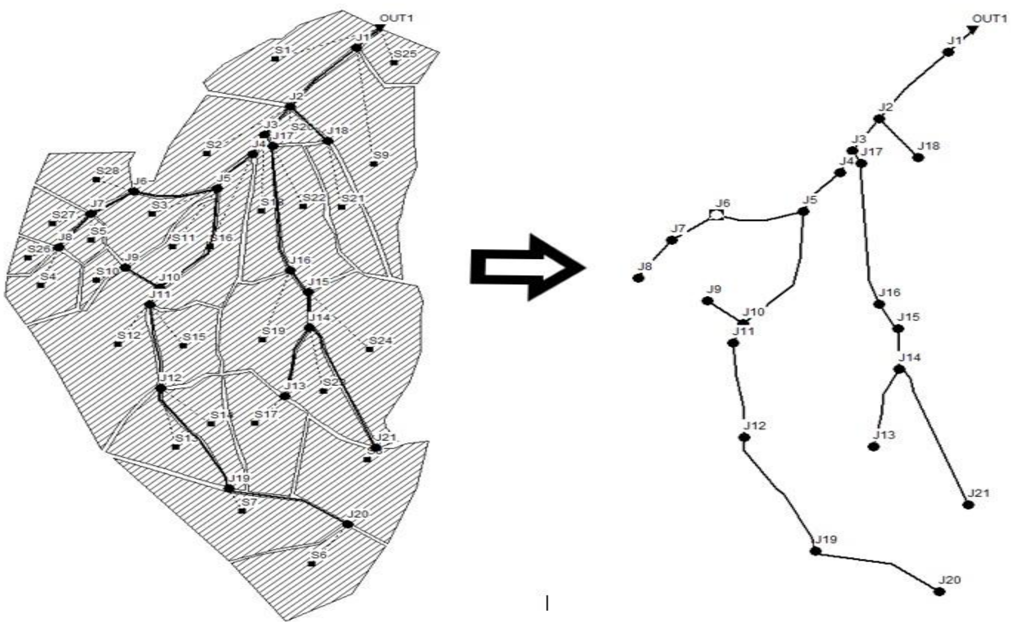


**Figure 4.7**. *Location of junctions in the study area map*

For the links, storm water pipes are considered conduits in this project. Two types of rainwater network, which were constructed at different times, were used. The second one was constructed after the May 2018 flood event. It will be used for comparison purposes in this project later.

Conduit properties include the shape of the pipe, maximum depth (diameter for circular shape), roughness coefficient, which depends on the material made and the length of the pipe. In these projects, there are 17 conduits that connect the highest point of the catchment to the outfall. The summary of all these properties of pipe networks is also given in Table 4.7.

**Table 4.7.** *Conduit properties for both previous and current draimage networks*

| **Conduit** | Length | Diameter previous (mm) | Diameter Current (mm) | Material made | n-manning |
|---|---|---|---|---|---|
| C1 | 180 | 400 | 1600 | Concrete | 0.012 |
| C2 | 404 | 400 | 1600 | Concrete | 0.012 |
| C3 | 168 | 400 | 2400 | Concrete | 0.012 |
| C4 | 216 | 400 | 1400 | Concrete | 0.012 |
| C5 | 100.42 | 500 | 400 | Concrete | 0.012 |
| C6 | 81.52 | 600 | 600 | Concrete | 0.012 |
| C7 | 723.52 | 1800 | 1800 | Concrete | 0.012 |
| C8 | 143.19 | 1600 | 1600 | Concrete | 0.012 |
| C9 | 175.39 | 1600 | 1600 | Concrete | 0.012 |
| C10 | 356.92 | 800 | 800 | Concrete | 0.012 |
| C11 | 717.48 | 1200 | 1200 | Concrete | 0.012 |
| C12 | 283.69 | 300 | 2000 | Concrete | 0.012 |
| C13 | 629.12 | 1800 | 1800 | Concrete | 0.012 |
| C14 | 107.47 | 1600 | 1600 | PVC | 0.009 |
| C15 | 503.35 | 1400 | 1400 | PVC | 0.009 |
| C16 | 599.42 | 800 | 800 | Concrete | 0.012 |
| C17 | 510 | 300 | 300 | Concrete | 0.012 |
| C18 | 184.19 | 400 | 400 | Concrete | 0.012 |
| C19 | 314.64 | 400 | 1400 | Concrete | 0.012 |
| C20 | 197.73 | 300 | 1000 | Concrete | 0.012 |
| C21 | 244.62 | 300 | 1000 | Concrete | 0.012 |

#### *4.2.1.4. Analysis Option*

The last thing before starting the simulation is setting the rest subcatchment and channel parameters and establishing analysis option for the model. Basin parameters include roughness coefficients, depression stores, and infiltration parameters. Pipe parameters include the roughness coefficient of the pipe, depending on the material from which the pipe is prepared. Modified Green Ampt will be used as an infiltration method in the subcatchment since it contains fewer parameters than other infiltration methods. Brown soils are dominantly found in the study area. These soils are zonal soils with ABC profile consisting of various main materials. Calcification plays a role in their formation. As a result of this process, there is a large amount of calcium in their profiles. A and C horizons are seen in those exposed to erosion.The value for suction head, conductivity, and intial defict is 3.5, 0.5, and 0.25, respectively. Dynamic wave will be used as routing method and the summary for whole anlysis option shown in Table 4.6.

**Table 4.8.** *Analysis option of the project*

| Option | Event-1 Value | Event-2 Value | Design Storms Value |
|---|---|---|---|
| **Flow units** | CMC | CMC | CMC |
| **Method of Routing** | Dynamic wave | Dynamic wave | Dynamic wave |
| **Start anlysis time and date** | 05/20/2018-13:00 | 06/09/2021-04:00 | 06/09/2021-00:00 |
| **Start reporting time and date** | 05/20/2018-13:00 | 06/09/2021-04:00 | 06/09/2021-00:00 |
| **End anlysis time and date** | 05/20/2018-20:00 | 06/09/2021-16:00 | 06/10/2021-00:00 |
| **Reporting time step** | 15 minute | 30 minute | 30 minute |
| **Routing time step** | 15 minute | 30 minute | 30 minute |

## 4.3. Modeling Peak Runoff Using Rational Equation

In this method, it is assumed that precipitation and direct flow have a linear connection; that is, the flow coefficients do not vary over time and precipitation falls uniformly throughout the whole drainage area. As a function of the catchment area, runoff coefficient, and average rainfall intensity for a duration equal to the time of concentration, the rational formula predicts the peak runoff at every point in a catchment area.

Time of concentration is the time taken for runoff to travel from the most remote point of the catchment to the drainage structure. There are a number of empirical equations available for the estimation of the time of concentration. Based on the Kirpich equation (1940), most of the time of concentration for each subcatchment is less than 5 minutes. Therefore, the minimum time of concentration value of 5 minutes used to read rainfall intensity values from IDF curve for peak discharge estimation. The maximum flow rate that will occur is estimated using the formula: **$Q_p$ =0.0028* C r A,** where '$Q_p$' denotes the peak flow rate (mm/hr), 'C' is the surface flow coefficient, 'r'= Rainfall (mm/hr), and 'A' is the area of drainage (in hectares).

Although the rational method produces satisfactory results in catchments up to 1–1.5 $km^2$, it may also be employed in drainage basins up to 5 $km^2$ (Hassen, 2016). In this project, a rational method is applied to a 10-year return period storm with a duration of 24 hours to estimate the peak discharge and compare it to the EPA SWMM result. This 10-year period storm just selected randomly for calibration purposes with SWMM.

## 5. RESULT AND ANALYSIS

### 5.1. RESULTS

### 5.1.1. EPA SWMM simulation results for drainage networks

#### *5.1.1.1. Scenario-I (event 1- old drainage)*

The name "Event-1" refers to the May 20th, 2018 rainfall data. Under these conditions, the simulation results seem to be of acceptable quality. For runoff and flow routing, the continuity error is -0.22 percent and 0.13 percent, respectively. This is far better than Rossman's limit, which states that a simulation is of inadequate quality if the continuity error exceeds 10% (Rossman, 2010).

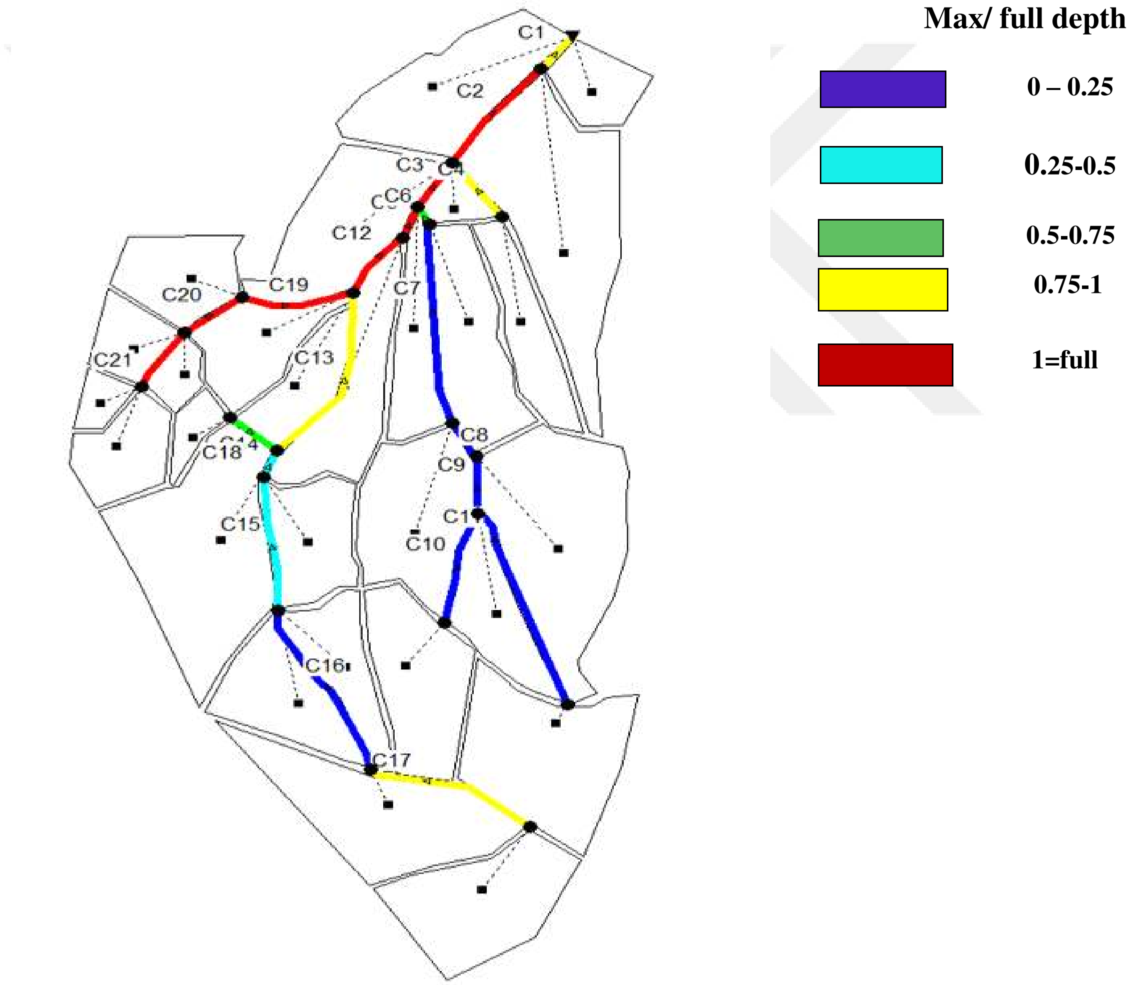


**Figure 5.1.** *Flow capacities of conduits in scenario I*

Channels C21, C20, C19, C12, C6, C3, and C2 overflowed due to inadequate channel sufficient to accommodate flow, as seen in Figure 5.1. As a result, the adjacent junction is overflown.

### *5.1.1.2. Scenario-II (Event 1- Current drainage)*

Runoff and flow routing continuity errors were -0.22 percent and -0.08 percent, respectively, indicating a relatively excellent simulation quality. As seen in Figure 5.2, all condites can handle flow without overflowing.

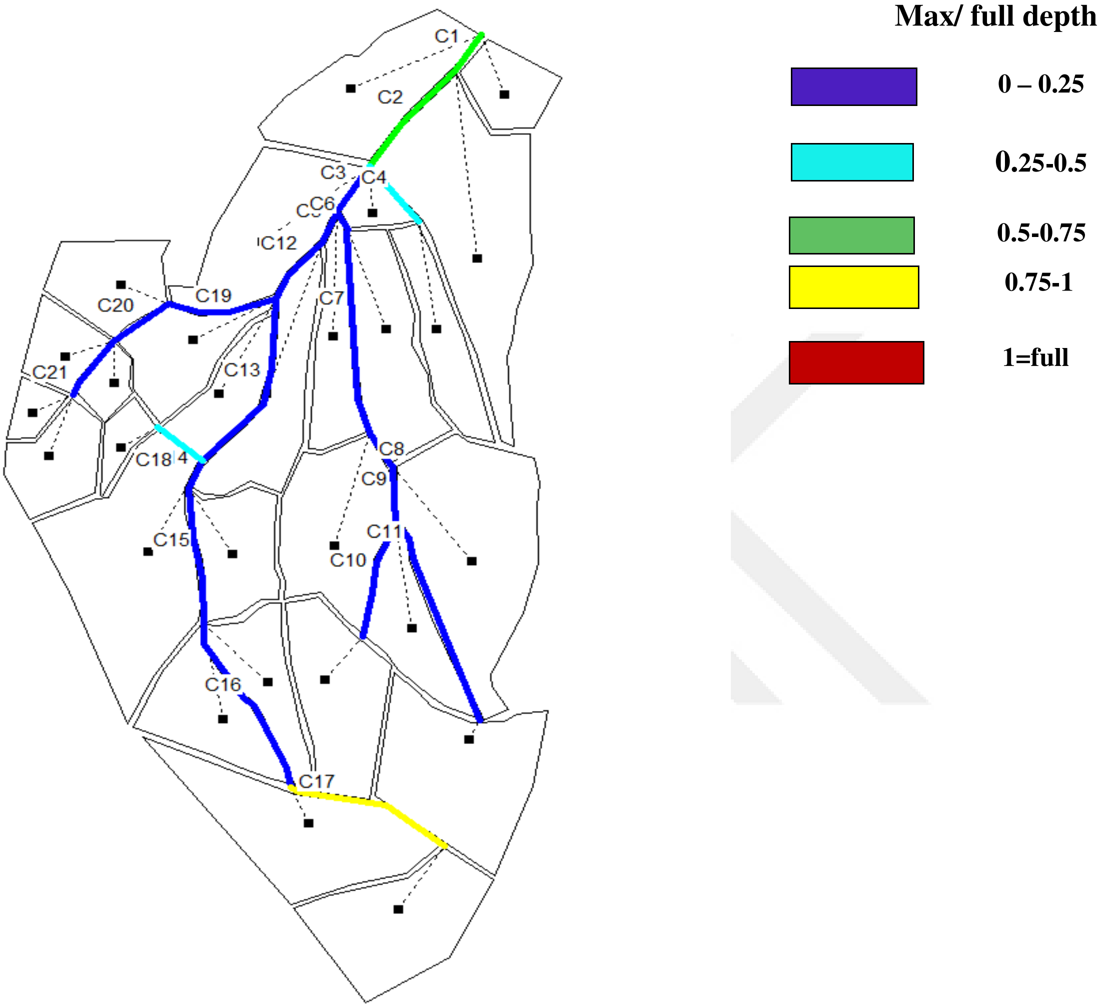


**Figure 5.2.** *Flow capacities of conduits in scenario II*

### *5.1.1.3. Scenario-III (event 2- Current drainage)*

The name "Event-2" refers to the June 9th, 2011 rainfall data. It is a rainfall event just happened recently on current drainage system. Continuity errors for runoff and flow routing were equivalent to -1.73 percent and 0.52 percent, in this simulation, indicating a relatively excellent simulation quality. All conduites, as seen in Figure 5.2, are capable of supporting flow without overflowing.

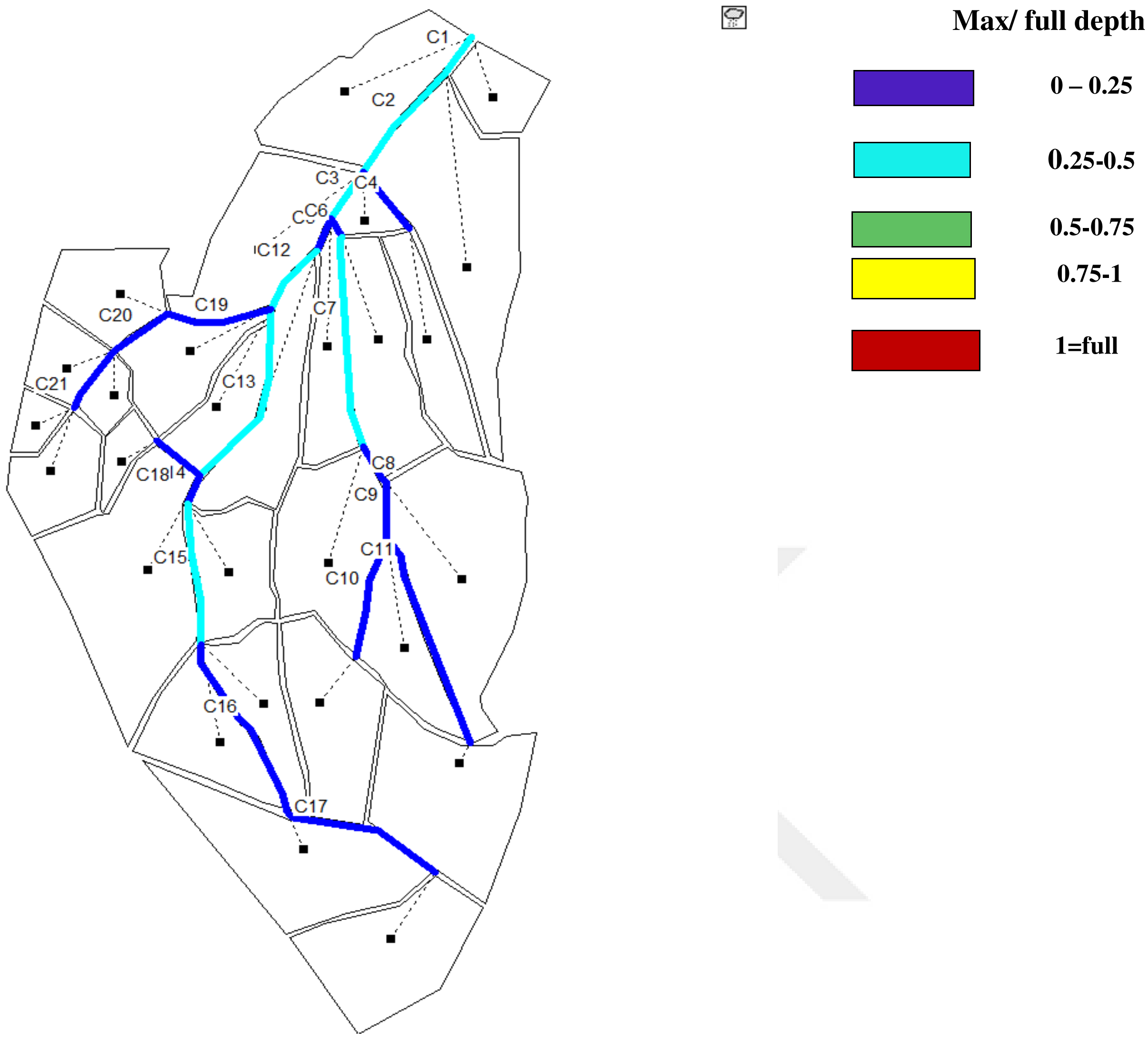


**Figure 5.3.** *Flow capacities of conduits in scenario III*

### 5.1.2. EPA SWMM Simulation Results for Drainage Nodes (Junctions)

The overflow time at each junction in the first two scenarios can be compared by reviewing the SWMM results. This is seen in Table 5.1. This is a simple explanation of how drainage systems influence flood simulation. For scenario 3, there is no overflown junction. Changes in drainage networks can have a significant impact on flood patterns. Figure 5.4 also illustrates a comparison of total outfall inflow between scenarios I and II. In scenario I, the majority of the precipitation flow is lost due to infiltration and floods (surface runoff). As there is no flooding in scenario II, the only flow losses are due to infiltration. As a result, scenario- II has a higher total inflow in outfall than scenario- I.

**Table 5.1.** *Flood hours comparison between scenario-I and scenario-II*

| Junction No | Hours Flooded | |
|---|---|---|
| | Scenario I | Scenario II |
| J1 | 5.19 | |
| J2 | 4.81 | |
| J3 | 4.67 | |
| J4 | 1.01 | |
| J5 | 4.66 | |
| J6 | 0.9 | |
| J7 | 1.02 | |
| J8 | 0.5 | |
| J9 | | |
| J10 | | |
| J11 | | |
| J12 | | |
| J13 | | |
| J14 | | |
| J15 | | |
| J16 | | |
| J17 | | |
| J18 | | |
| J19 | | |
| J20 | 1.02 | 0.92 |
| J21 | | |

Flooded nodes

For scenario 1 and 2, Figure 5.4 displays the hydrograph for total input overflow at the catchment's outlet. Since there is no surface runoff or flooding in scenario 2, it’s total inflow at outfall is much greater than scenario1.

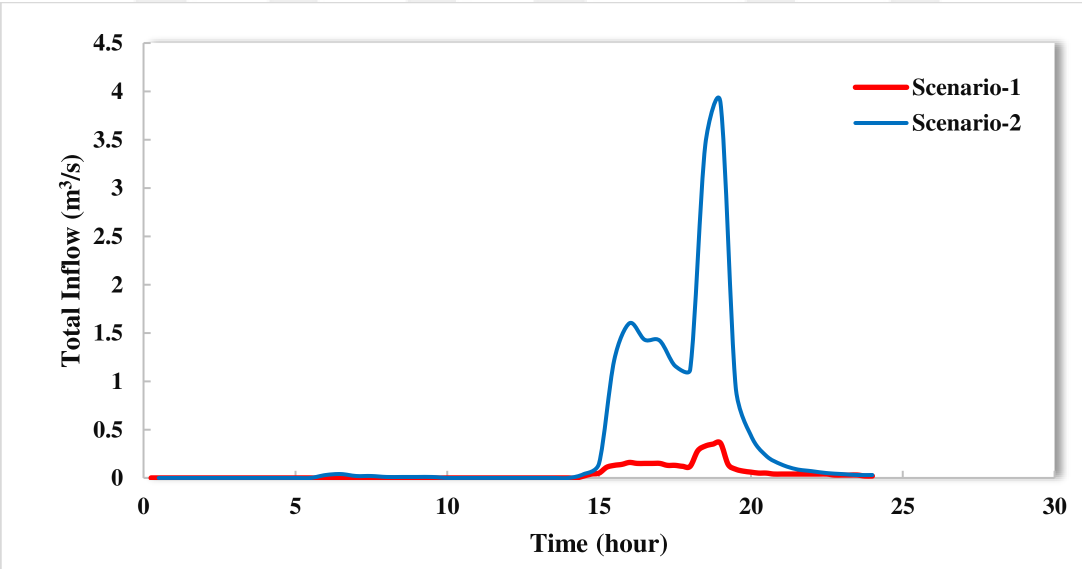


**Figure 5.4.** *Comparison of Outfall hydrographs between Scenario-1 and Scenario-2*

The channel C19, shown in Figure 5.5, that links nodes J6 and J5, is at its maximum capacity. When the channel is full with water, the next node (J5) overflows due to the pressure of the pipeline flow.

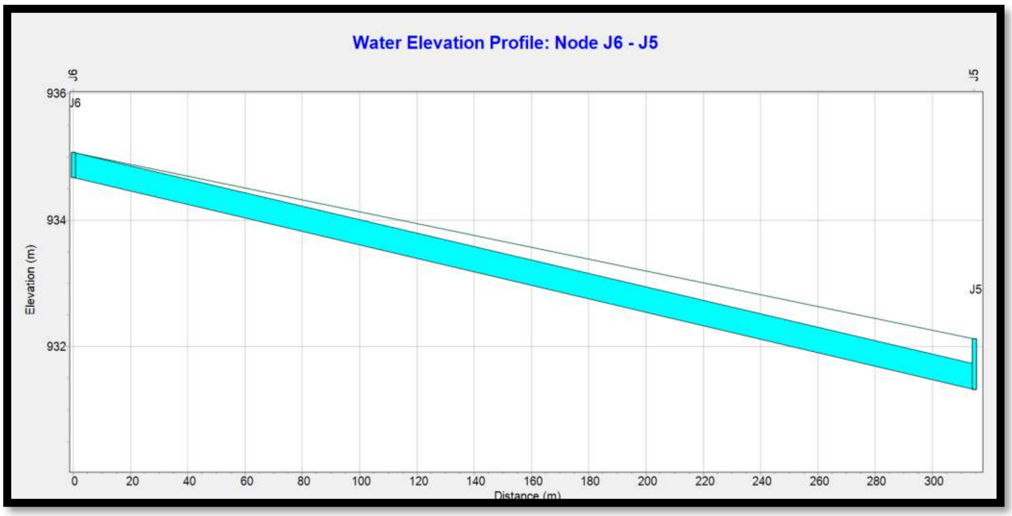


**Figure 5.5.** *Water Elevation profile: Node J6-J5 for scenario-1*

Figure 5.6 demonstrates the same condition as in scenario 2. As the conduit (C19) connecting nodes J6 and J5 is not at its full capacity, an overflow in node J5 close to it was prevented. Only a tenth of the pipeline's capacity was used. This happened as result of the pipeline size change in scenario 2. As there is no flooding in scenario 3, the situation will be thes same as scenario 2.

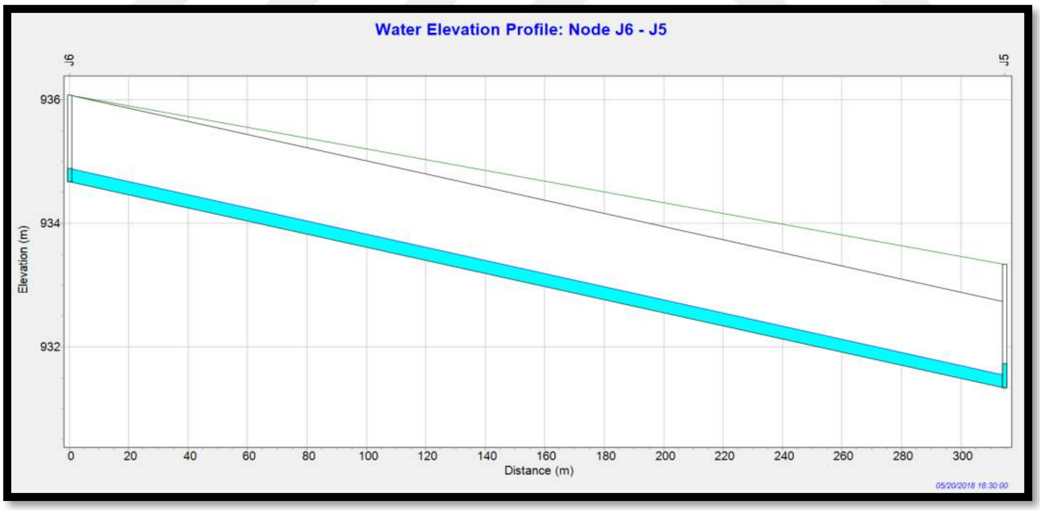


**Figure 5.6.** *Water Elevation profile: Node J6-J5 for scenario-2*

When the May 2018 flood hit the Mamak Boğaziçi neighborhood, the Neşet Ertaş street that connects J8 node to the outlet of the catchment was one of the worst-hit areas. In this location, there was no reliable drainage system at the area. Figure 5.7 displays the actual flooding that occurred as a result of the drainage system's overflow. Referring to the figure, the pressure pipeline flow inundated all junctions.

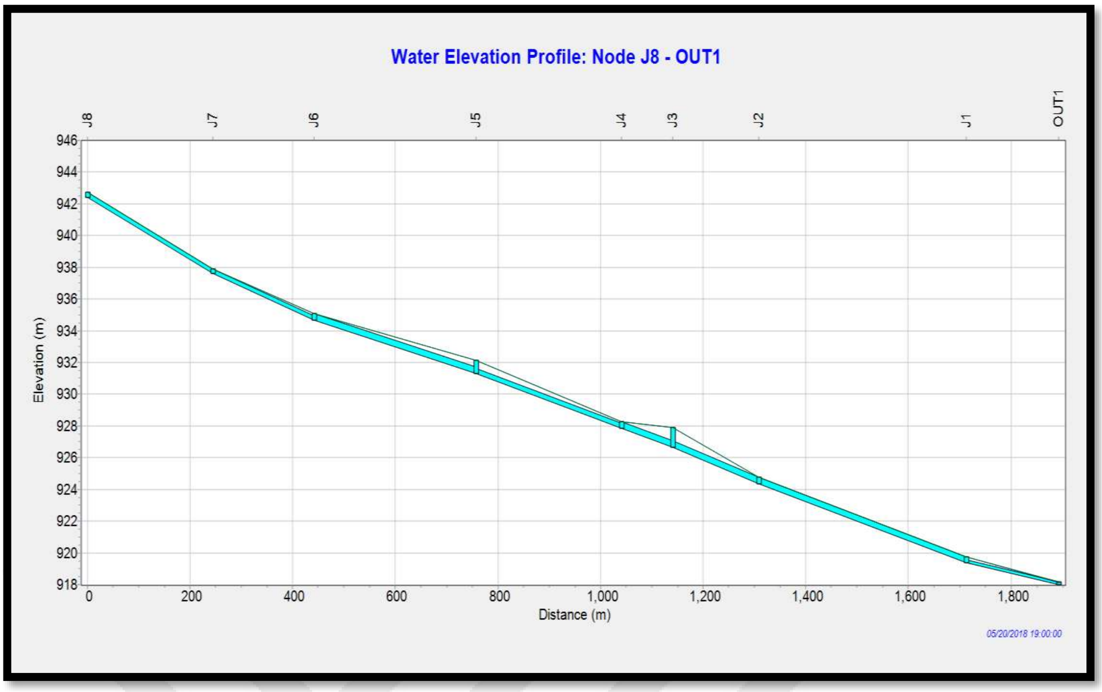


**Figure 5.7.** *Water Elevation profile: Node J8-outfall for scenario-1 (Neşet Ertaş street).*

Table 5.2 summarizes the parameters of node flooding, including hours of flooding, maximum rate ($m^3/s$), days of maximum flooding, maximum flooding hours, total flood volume ($10^3$ $m^3$), and maximum ponded depth (meters) for scenario 1. Figure 5.8 represents the total flood volume in the catchment's inundated junction of scenario 1. As J5 is a common junction for 2 separate conduits, it is the most overflowed junction with a total flood volume of $12.802\times 10^3$ $m^3$.

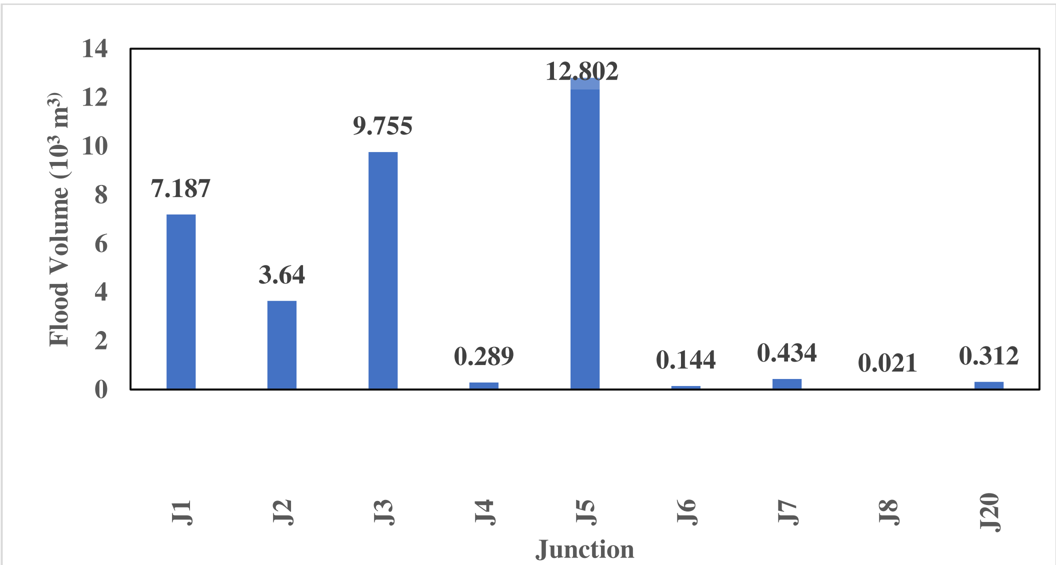


**Figure 5.8**. *Total flood volume for overflowed junctions in scenario 1*

**Table 5.2.** *Summary for Node Flooding in SWMM (scenario 1)*

| Node | Hours Flooded | Maximum rate ($m^3/s$) | Days of Maximum Flooding | Hour of Maximum flooding | Total Flood Volume ($10^3$ $m^3$) | Maximum ponded Depth (meters) |
|---|---|---|---|---|---|---|
| J1 | 5.19 | 0.673 | 0 | 6:00 | 7.187 | 0 |
| J2 | 4.81 | 0.476 | 0 | 6:00 | 3.64 | 0 |
| J3 | 4.67 | 1.513 | 0 | 6:00 | 9.755 | 0 |
| J4 | 1.01 | 0.095 | 0 | 6:00 | 0.289 | 0 |
| J5 | 4.66 | 1.729 | 0 | 6:00 | 12.802 | 0 |
| J6 | 0.9 | 0.053 | 0 | 6:00 | 0.144 | 0 |
| J7 | 1.02 | 0.142 | 0 | 6:00 | 0.434 | 0 |
| J8 | 0.5 | 0.017 | 0 | 6:00 | 0.021 | 0 |
| J20 | 1.02 | 0.123 | 0 | 6:00 | 0.312 | 0 |

### 5.1.3. EPA SWMM simulation results for design precipitation

Using the model setup above, flood processes with varied return durations and design precipitation were simulated for 24-hr duration. Figure 5.9 displays the discharge at the outlet for different return periods. The results cannot be independently verified for the reason that they are based on design rainfall.

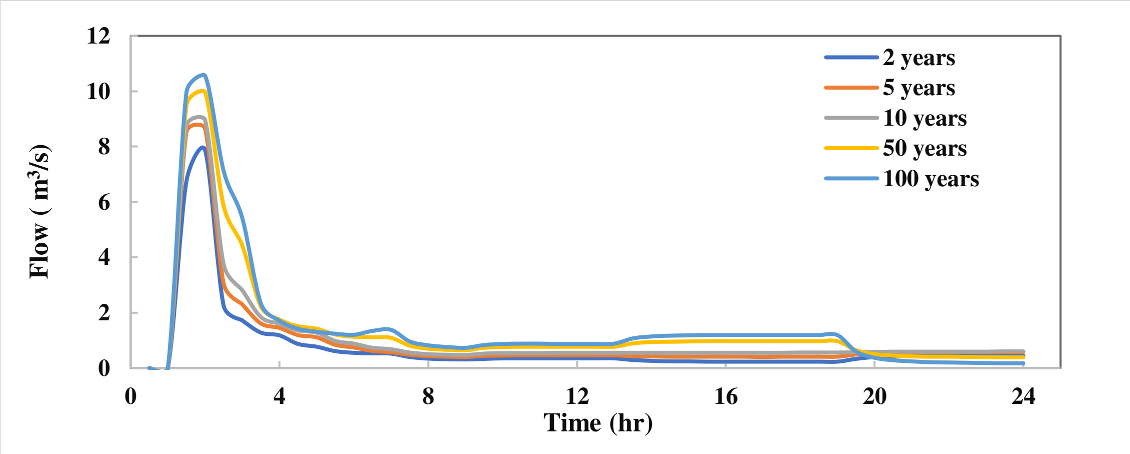


**Figure 5.9**. *Simulated discharge of different return periods at the outlet.*

For 2-year return period storm only J1 will be flooded, and the amount of flood volume is significantly low. Only J1 and J2 will be inundated in case of 5, 10, and 50-year return period. For 100-year return period five junctions namely J1, J2, J4 and J5 will be flooded. J3, which was one of the most overflowded junction in old drainage was not flooded in current drainage sysytem as the C3 (J3-J2) conduit's diameter changed in large extent compared to other junctions as shown earlier in Table 4.7.

### 5.1.4. Results for rational method

Peak discharge in the research area's sub-catchments over a ten-year return period was estimated using the rational formula. The comparison of peak discharge in all subcatchments between the EPA SWMM and rational method summarized in Table 5.3.

**Table 5.3.** *Summary for Peak discharge*

| Sub-ID | Area (ha) | Rnfall intensity (mm/hr) | Runoff coefficient | $Q_p$ ($m^3/s$) (Rational) | $Q_p$ ($m^3/s$) (EPA SWMM) |
|---|---|---|---|---|---|
| **S1** | 16.3 | 48.1 | 0.53 | 1.16 | 1.22 |
| **S2** | 16.9 | 48.1 | 0.45 | 1.02 | 1.25 |
| **S3** | 9.58 | 48.1 | 0.70 | 0.90 | 0.72 |
| **S4** | 7.91 | 48.1 | 0.63 | 0.68 | 0.59 |
| **S5** | 2.75 | 48.1 | 0.61 | 0.23 | 0.21 |
| **S6** | 16.4 | 48.1 | 0.58 | 1.29 | 1.2 |
| **S7** | 19.3 | 48.1 | 0.56 | 1.47 | 1.42 |
| **S8** | 21 | 48.1 | 0.55 | 1.56 | 1.47 |
| **S9** | 28.4 | 48.1 | 0.70 | 2.68 | 2.14 |
| **S10** | 2.61 | 48.1 | 0.70 | 0.25 | 0.2 |
| **S11** | 7.43 | 48.1 | 0.45 | 0.45 | 0.56 |
| **S12** | 28.1 | 48.1 | 0.75 | 2.84 | 2.12 |
| **S13** | 11.1 | 48.1 | 0.95 | 1.42 | 0.84 |
| **S14** | 8.54 | 48.1 | 0.75 | 0.65 | 0.65 |
| **S15** | 9.64 | 48.1 | 0.75 | 0.97 | 0.73 |
| **S16** | 12.3 | 48.1 | 0.66 | 1.09 | 0.93 |
| **S17** | 14.9 | 48.1 | 0.70 | 1.12 | 1.12 |
| **S18** | 8.41 | 48.1 | 0.45 | 0.51 | 0.63 |
| **S19** | 16.7 | 48.1 | 0.70 | 1.57 | 1.26 |
| **S20** | 2.41 | 48.1 | 0.70 | 0.23 | 0.18 |

| | | | | | |
|---|---|---|---|---|---|
| **S21** | 9.2 | 48.1 | 0.75 | 0.93 | 0.7 |
| **S22** | 14.2 | 48.1 | 0.45 | 0.86 | 1.07 |
| **S23** | 9.32 | 48.1 | 0.75 | 0.94 | 0.71 |
| **S24** | 27.6 | 48.1 | 0.58 | 2.14 | 2 |
| **S25** | 4.13 | 48.1 | 0.30 | 0.17 | 0.3 |
| **S26** | 2.37 | 48.1 | 0.70 | 0.22 | 0.18 |
| **S27** | 4.67 | 48.1 | 0.70 | 0.44 | 0.35 |
| **S28** | 9.51 | 48.1 | 0.70 | 0.90 | 0.72 |

Figure 5.10 shows the Comparison of peak discharges between EPA-SWMM and Rational methods for 10-year return period. This data will later used For model evaluation.

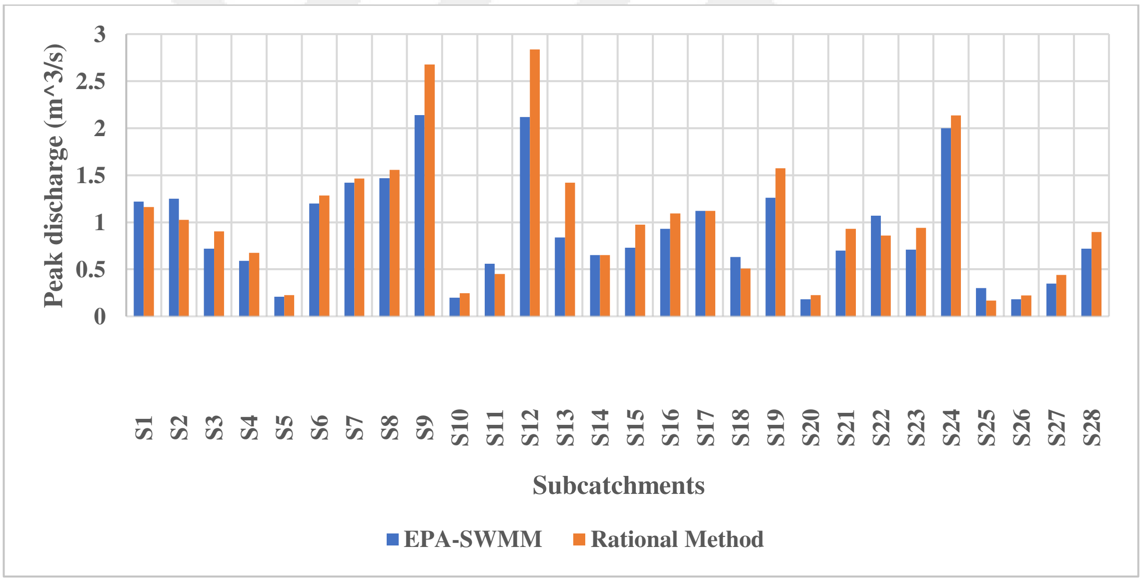


**Figure 5.10.** *Comparison of peak discharges between EPA-SWMM and Rational methods for 10-year return period.*

## 5.2. Model Evaluation with Efficiency Criterias

The efficiency criterias that used for model evaluation of this project includes the Nash and Sutcliffe efficiency, index of agreement and Root-Mean Square Error (RMSE).

The result for Nash and Sutcliffe Efficiency measure that connects the model's goodness-of-fit to the variance of measured data is 0.867. NSE values ranging from 0.9

to 1 suggest that the model works exceptionally well, while values ranging from 0.6 to 0.8 indicate that the model performs quite well(Nash & Sutcliffe, 1970)

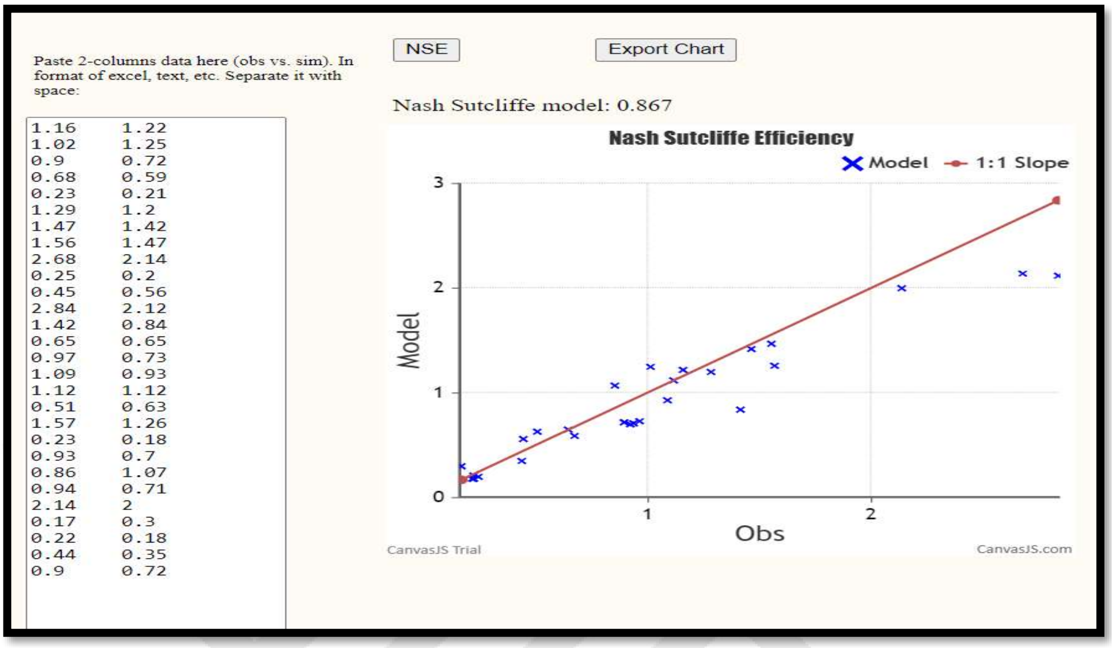


**Figure 5.11**. *NSE result for the model*

The result for an index of agreement (d) is a standardized measure of model prediction error ranging from 0 to 1 is 0.959 as shown in Figure 5.12. A score of 1 shows a perfect match, whereas a value of 0 indicates no agreement at all.

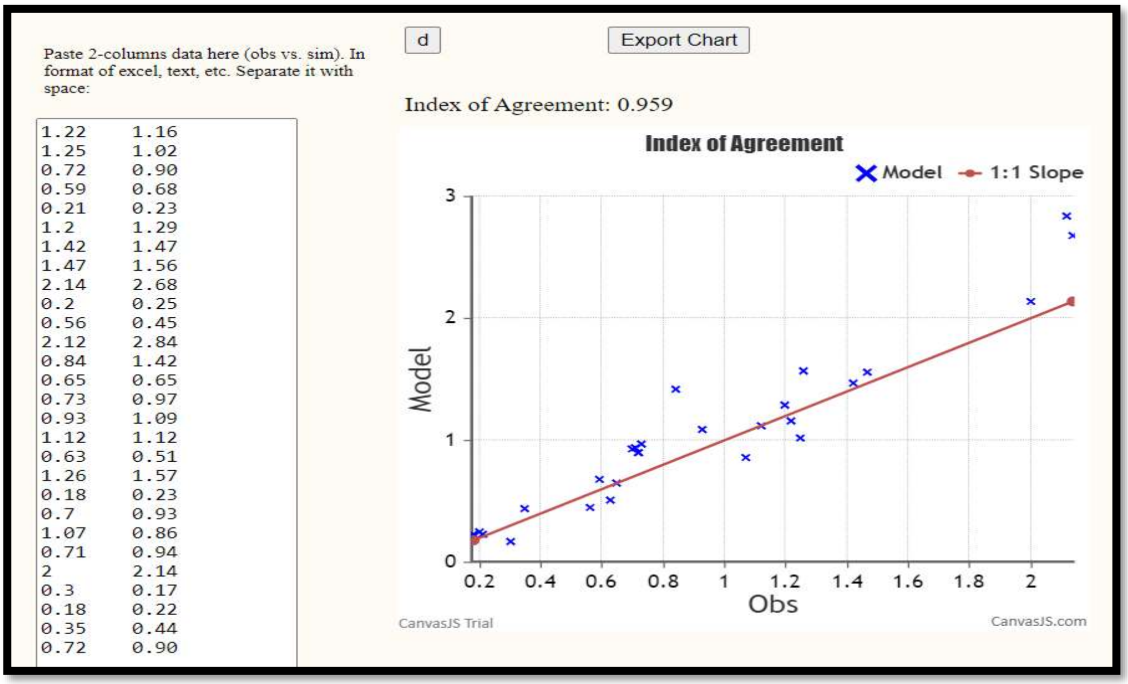


**Figure 5.12**. *Model's index of agrrement*

The result for R-squared correlation coefficient is 0.916 which indicates that the model performance is good.

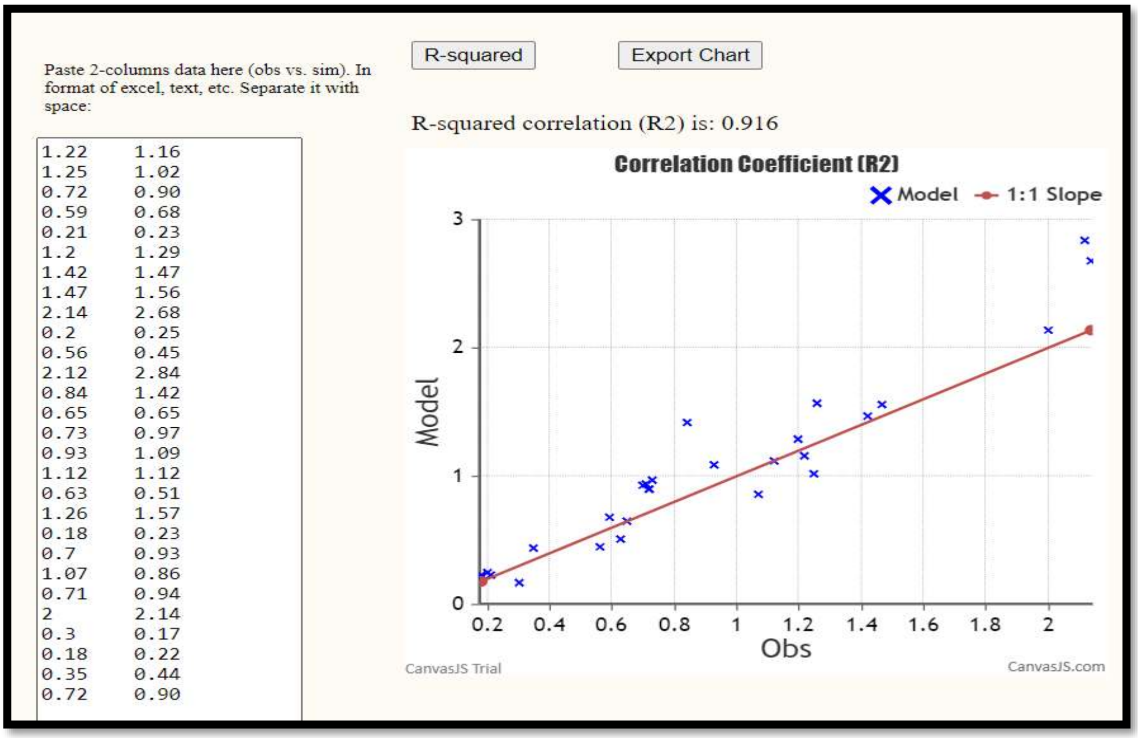


**Figure 5.13**. *Model's R-squared correlation coefficient.*

**Table 5.4.** *Performance evaluation of Efficency criterias*

| Efficency criterias | Value | Performance Evaluation |
|---|---|---|
| **NSE** | 0.867 | Good |
| **Index of Agreement (d)** | 0.959 | Excellent |
| **$R^2$** | 0.916 | Excellent |

# 6. CONCLUSION

The EPA SWMM software program was used to simulate event-based rainfall-runoff flood modeling for the Boğaziçi area of Mamak district, Ankara, based on previous and present drainage networks. Furthermore, the present drainage system was simulated for design storms with return periods of 2, 5, 10, 50, and 100 years. To examine the responsiveness of the drainage network, three alternative scenarios were run with two different rainfall events. The first and second scenarios mimicked a historic rainfall event that happened in May 2018 for both previous and present drainage networks.

The primary reason for mapping this research region is that it is usually vulnerable to floods during the rainy season due to the terrain and insufficient drainage infrastructure. Flooding has been particularly severe in the neighborhood's Neşet Ertaş street. The second explanation is that the existing drainage networks were built right after the May 2018 rainfall storm, according to pipeline data. The present drainage system was then modeled using a recent rainfall event that occurred in June 2021 to evaluate its effectiveness.

The rational method of estimating peak discharge was also used to calculate peak flows in each of the study area's subcatchments. For the design storm, this calculated peak flow was applied for calibration with a 10-year return period of 24 hours. Model evaluation was done using calculated and simulated peak flows to determine the model's accuracy and reliability. To assess the hydraulic behavior and performance of the model, several efficiency measures such as Nash and Sutcliffe efficiency, coefficient of determination, and index of agreement were performed.

The results of three alternative scenarios, based on different indexes for urban flood forecasting, demonstrate that the fundamental problem with earlier drainage was an insufficient drainage infrastructure. In previous drainage networks, the conduits connecting J8 to the study area's outfall, which is located on Neşet Ertaş street, were subjected to pressurized pipeline flow, causing the nearby junctions to overflow. In urban flood simulation, pressured pipeline flow is an important index. The only approach is to reduce the volume of water entering the conduits or to enlarge the conduit itself, which is hardly cost-effective. The rainwater network has already been enlarged the scope of this incident. The second scenario demonstrates how essential drainage networks are in urban floods since it produces varied results for the same rainfall event and study area.

Another index in urban flood modelling is the total inflow in the outfall of the study area. As shown in Figure 5.4, the total outlet discharge in scenario-2 is significantly greater than scenario-1. This is because most of the flow in scenario-1 was lost due to overflown junctions. This is the best example to demonstrate the effect of drainage system in urban flood modelling.

Due to the fact that the existing drainage system did not experience floods during historical occurrences, it had to be modelled using synthetic storms. Even though synthetic storms are recorded based on historical rainfall occurrences, they are critical tools for flood forecasting. The present drainage system was modeled using 2, 5, 10, 50, and 10-year return period design storms with a 24-hour duration based upon Ankara's IDF curve. Only J1 will be inundated during the two-year return period storm, and the flood volume will be rather little. In the event of a 5, 10, or 50-year return period, only J1 and J2 will be flooded. Four junctions, namely J1, J2, J4, and J5, will be inundated during the 100-year return period.

The Rational method was used to estimate peak discharge of 10-year return period storm event for comparison reasons. This approach is applicable to drainage regions ranging up to 5 $km^2$. The model was evaluated using calculated values from the rational approach and simulated values from SWMM. The Nash and Sutcliffe efficiency coefficient was 0.867, indicating that the model worked effectively. The agreement index was 0.959, which is quite near to one and indicates a perfect match. The $R^2$-coefficient was 0.916, indicating that the model was eiificently good.

Finally, various abnormalities, ambiguities, and excesses in precipitation over the last several years have been attributed to excessive reliance on fossil fuels, increasing carbon emissions, and climate change. It is possible to reduce the risk of flooding, particularly in urban areas, by implementing various LID control strategies, such as increasing green areas to ensure maximum infiltration rates.

# REFERENCES

Agarwal, S., & Kumar, S. (2020). *Urban Flood Modeling using SWMM for Historical and Future Extreme Rainfall Events under Climate Change Scenario Academic View project Storm Water Management Model (SWMM) View project*. https://www.researchgate.net/publication/343905044

AgriMetSoft. (n.d.). *R-squared Calculator*. 2019. Retrieved April 3, 2022, from https://agrimetsoft.com/calculators/R-squared%20correlation

Badham, J., Elsawah, S., Guillaume, J. H. A., Hamilton, S. H., Hunt, R. J., Jakeman, A. J., Pierce, S. A., Snow, V. O., Babbar-Sebens, M., Fu, B., Gober, P., Hill, M. C., Iwanaga, T., Loucks, D. P., Merritt, W. S., Peckham, S. D., Richmond, A. K., Zare, F., Ames, D., & Bammer, G. (2019). Effective modeling for Integrated Water Resource Management: A guide to contextual practices by phases and steps and future opportunities. *Environmental Modelling & Software*, *116*, 40–56. https://doi.org/10.1016/j.envsoft.2019.02.013

Ceylan, A., Ayvaci, H., Akgündüz, S., Hüküm, H., & Güser, Y. (2015). *ŞEHİR SELLERİ TAHMİN VE ERKEN UYARI MODELİ *Meteoroloji Genel Müdürlüğü, Araştırma Dairesi Başkanlığı Kalaba/ANKARA*. https://www.mgm.gov.tr/FILES/genel/makale/sehirselleri_atmos.pdf

EM-DAT. (2012). *EM-DAT | The international disasters database*. https://www.emdat.be/

Gordon, S. I. (1985). Models in Environmental Planning. In *Computer Models in Environmental Planning* (pp. 1–13). Springer US. https://doi.org/10.1007/978-1-4684-6590-7_1

Goren, A., & Goksu, F. (2018). *Mamak'ı sel vurdu - Ankara Başkent Haberleri*. https://www.sabah.com.tr/ankara-baskent/2018/05/06/mamaki-sel-vurdu-1525589662

Gupta, H. v., Bastidas, L. A., Vrugt, J. A., & Sorooshian, S. (2003). *Multiple criteria global optimization for watershed model calibration* (pp. 125–132). https://doi.org/10.1029/WS006p0125

Haris, H., Chow, M. F., Usman, F., Sidek, L. M., Roseli, Z. A., & Norlida, M. D. (2016). Urban Stormwater Management Model and Tools for Designing Stormwater Management of Green Infrastructure Practices. *IOP Conference Series: Earth and Environmental Science*, *32*, 012022. https://doi.org/10.1088/1755-1315/32/1/012022

Hassen, N. (2016). *MODELING AND ANALYSES OF URBAN FLOODING IN BOLE SUBCITY SYSTEM PERFORMANCE AND EVALUATION OF POSSIBLE IMPROVEMENTS USING EP SWMM5*.

Huber, W. C., & Barnwell, T. O. (1988). *STORM WATER MANAGEMENT MODEL, VERSION 4: USER'S MANUAL*.

Jiang, L., Chen, Y., & Wang, H. (2015). Urban flood simulation based on the SWMM model. *Proceedings of the International Association of Hydrological Sciences*, *368*, 186–191. https://doi.org/10.5194/piahs-368-186-2015

Junaidi, Ermalizar, L. M., & Junaidi, A. (2018). Flood simulation using EPA SWMM 5.1 on small catchment urban drainage system. *MATEC Web of Conferences*, *229*, 04022. https://doi.org/10.1051/matecconf/201822904022

Kömüşcü, A. Ü., & Çelik, S. (2013). Analysis of the Marmara flood in Turkey, 7–10 September 2009: an assessment from hydrometeorological perspective. *Natural Hazards*, *66*(2), 781–808. https://doi.org/10.1007/s11069-012-0521-x

Kourtis, I. M., Kopsiaftis, G., Bellos, V., & Tsihrintzis, V. A. (2017). *Calibration and validation of SWMM model in two urban catchments in Athens, Greece Municipal sludge dewatering using Sludge Treatment Wetlands View project Calibration and validation of SWMM model in two urban catchments in Athens, Greece*. https://www.researchgate.net/publication/319465255

Lv, G., Xiong, L., Chen, M., Tang, G., Sheng, Y., Liu, X., Song, Z., Lu, Y., Yu, Z., Zhang, K., & Wang, M. (2017). Chinese progress in geomorphometry. *Journal of Geographical Sciences*, *27*(11), 1389–1412. https://doi.org/10.1007/s11442-017-1442-0

Nanduri, U. v, Patel, A., Rangari, V. A., Prashanth, S. S., Umamahesh, N. v, Patel, A. K., Scholar, R., & Student, G. (2018). Simulation of Urban Drainage System using a Storm Water Management Model (SWMM). In *Asian Journal of Engineering and Applied Technology* (Vol. 7, Issue S1). https://www.researchgate.net/publication/323993331

Nash, J. E., & Sutcliffe, J. V. (1970). River flow forecasting through conceptual models part I — A discussion of principles. *Journal of Hydrology*, *10*(3), 282–290. https://doi.org/10.1016/0022-1694(70)90255-6

Öner, S. (1997). *The Use of SWMM simulation model in urban storm water management*.

Ponce, V. M., & Hawkins, R. H. (1996). Runoff Curve Number: Has It Reached Maturity? *Journal of Hydrologic Engineering*, *1*(1), 11–19. https://doi.org/10.1061/(ASCE)1084-0699(1996)1:1(11)

Rana, V. K., & Suryanarayana, T. M. V. (2020). GIS-based multi criteria decision making method to identify potential runoff storage zones within watershed. *Annals of GIS*, *26*(2), 149–168. https://doi.org/10.1080/19475683.2020.1733083

Rosa, D. J., Clausen, J. C., & Dietz, M. E. (2015). Calibration and Verification of SWMM for Low Impact Development. *JAWRA Journal of the American Water Resources Association*, *51*(3), 746–757. https://doi.org/10.1111/jawr.12272

Rossman, L. A. (2010). Modeling Low Impact Development Alternatives with SWMM. *Journal of Water Management Modeling*. https://doi.org/10.14796/JWMM.R236-11

sen Zeytun, A., Çetinkaya, B., & ERBAS, A. K. (2016). Understanding Prospective Teachers' Mathematical Modeling Processes in the Context of a Mathematical Modeling Course. *EURASIA Journal of Mathematics, Science and Technology Education*, *13*(3). https://doi.org/10.12973/eurasia.2017.00639a

Steinman, A., Chu, X., & Ogdahl, M. (2009). Spatial and temporal variability of internal and external phosphorus loads in Mona Lake, Michigan. *Aquatic Ecology*, *43*(1), 1–18. https://doi.org/10.1007/s10452-007-9147-6

Sun, N., Hall, M., Hong, B., & Zhang, L. (2014). Impact of SWMM Catchment Discretization: Case Study in Syracuse, New York. *Journal of Hydrologic Engineering*, *19*(1), 223–234. https://doi.org/10.1061/(ASCE)HE.1943-5584.0000777

Toros, H., Kahraman, A., Tilev-Tanriover, S., Geertsema, G., & Cats, G. (2018). İstanbul'da 8-9 Eylül 2009'da Meydana Gelen Aşırı Yağışın HARMONIE, HIRLAM ve WRF-ARW ile Simülasyonu. *European Journal of Science and Technology*, 1–12. https://doi.org/10.31590/ejosat.417535

Waikar, M. L., & Namita, U. (2015). *Urban Flood Modeling by using EPA SWMM 5*. https://www.researchgate.net/publication/282655574

Wang, H.-W., Zhai, Y.-J., Wei, Y.-Y., & Mao, Y.-F. (2019). Evaluation of the effects of low-impact development practices under different rainy types: case of Fuxing Island Park, Shanghai, China. *Environmental Science and Pollution Research*, *26*(7), 6706–6716. https://doi.org/10.1007/s11356-019-04129-x

Wanniarachchi, S. S., & Wijesekera, N. T. S. (2012). Using SWMM as a Tool for Floodplain Management in Ungauged Urban Watershed. *Engineer: Journal of the Institution of Engineers, Sri Lanka*, *45*(1), 1. https://doi.org/10.4038/engineer.v45i1.6944

Willmott, C. J., Robeson, S. M., & Matsuura, K. (2012). A refined index of model performance. *International Journal of Climatology*, *32*(13), 2088–2094. https://doi.org/10.1002/joc.2419

Yu, H., Huang, G., & Wu, C. (2014). Application of the stormwater management model to a piedmont city: a case study of Jinan City, China. *Water Science and Technology*, *70*(5), 858–864. https://doi.org/10.2166/wst.2014.302

Zhang, B., Chen, M., Ma, Z., Zhang, Z., Yue, S., Xiao, D., Zhu, Z., Wen, Y., & Lü, G. (2022). An online participatory system for SWMM-based flood modeling and simulation. *Environmental Science and Pollution Research*, *29*(5), 7322–7343. https://doi.org/10.1007/s11356-021-16107-3

Zoppou, C. (2001). Review of urban storm water models. *Environmental Modelling & Software*, *16*(3), 195–231. https://doi.org/10.1016/S1364-8152(00)00084-0

# APPENDIX

## A-1. Parameter Units in SWMM

| PARAMETER | US CUSTOMARY | SI METRIC |
|---|---|---|
| Area (Subcatchment) | acres | hectares |
| Area (Storage Unit) | square feet | square meters |
| Area (Ponding) | square feet | square meters |
| Capillary Suction | inches | millimeters |
| Concentration | mg/L (milligrams/liter)<br>ug/L (micrograms/liter)<br>Count/L (counts/liter) | mg/L<br>ug/L<br>Count/L |
| Decay Constant (Infiltration) | 1/hours | 1/hours |
| Decay Constant (Pollutants) | 1/days | 1/days |
| Depression Storage | inches | millimeters |
| Depth | feet | meters |
| Diameter | feet | meters |
| Discharge Coefficient:<br>Orifice<br>Weir | <br>dimensionless<br>CFS/foot$^n$ | <br>dimensionless<br>CMS/meter$^n$ |
| Elevation | feet | meters |
| Evaporation | inches/day | millimeters/day |
| Flow | CFS (cubic feet / second)<br>GPM (gallons / minute)<br>MGD (million gallons/day) | CMS (cubic meters/second)<br>LPS (liters/second)<br>MLD (million liters/day) |
| Head | feet | meters |
| Hydraulic Conductivity | inches/hour | millimeters/hour |
| Infiltration Rate | inches/hour | millimeters/hour |
| Length | feet | meters |
| Manning's n | seconds/meter$^{1/3}$ | seconds/meter$^{1/3}$ |
| Pollutant Buildup | mass/length<br>mass/acre | mass/length<br>mass/hectare |
| Rainfall Intensity | inches/hour | millimeters/hour |
| Rainfall Volume | inches | millimeters |
| Slope (Subcatchments) | percent | percent |
| Slope (Cross Section) | rise/run | rise/run |
| Street Cleaning Interval | days | days |
| Volume | cubic feet | cubic meters |
| Width | feet | meters |

## CURRICULUM VITAE

Name Surname : Seid Dessalegn SHAFI

Foreign language : English, Arabic, and Turkish

Education History:

- ✓ 2022,Eskisehir Technical University, Hydraulics Dept.
- ✓ 2019, Eskisehir Osmangazi University, Civil Engineering Dept.